Effect of cloud cover and atmospheric circulation patterns on the observed surface solar radiation in Europe

Marc Chiacchio[1,2] and Renato Vitolo[3]

Received 12 February 2012; revised 3 August 2012; accepted 8 August 2012; published 22 September 2012.

[1] This study aims at quantifying the most important factors affecting variations in downward surface shortwave radiation (DSW) in Europe including cloud cover and atmospheric circulation patterns. The role of observed cloud cover on DSW was analyzed through generalized linear models using DSW measurements obtained from the Global Energy Balance Archive during 1971–1996. Stations of DSW in Europe were selected to assess how they were affected by clouds. Overall cloud cover had a statistically significant negative relationship and a non-significant positive relationship on DSW for relatively nearby and distant cloud cover stations, respectively. The exception was west-central Europe where a significant negative effect over the whole continent was found suggesting an association with larger cloud structures. This showed that point DSW measurements can be spatially representative for larger scale variability. In line with other studies we found a strong seasonal effect of cloud cover on DSW mainly in northern Europe in spring and summer and in southern Europe in winter and autumn. The North Atlantic Oscillation was most important in winter with a significant negative effect in northern to central Europe and a positive non-significant effect in the south. The Mediterranean Oscillation exhibited mainly a positive effect in winter with significance in southern Europe and non-significance in central Europe. The North Sea Caspian Pattern primarily showed a positive effect with significance in east-central and northern Europe in spring and summer. The interrelationship found between these climatic variables could improve the understanding of a linkage to temperature and precipitation patterns in Europe.

Citation: Chiacchio, M., and R. Vitolo (2012), Effect of cloud cover and atmospheric circulation patterns on the observed surface solar radiation in Europe, *J. Geophys. Res.*, *117*, D18207, doi:10.1029/2012JD017620.

1. Introduction

[2] Incoming solar radiation that reaches the surface of the Earth is the major source of energy in the climate system and is a major factor in regulating the surface energy balance. Any changes in this radiative balance could have dramatic effects on surface processes related to the hydrological and carbon cycles [*Liepert et al.*, 2004; *Wild and Liepert*, 2010; *Mercado et al.*, 2009] as well as its impact on surface temperature [*Ramanathan et al.*, 2001; *Wild et al.*, 2005, 2007]. Hence, the downward shortwave radiation (DSW) at the surface is a major component of the surface radiative balance which has now been studied extensively in recent years, particularly its decadal changes through time. Namely, a reduction (dimming) has been discovered from about the 1950s until about the 1980s in many parts of the world [*Gilgen et al.*, 1998; *Liepert*, 2002; *Stanhill and Cohen*, 2001] followed by an increase (brightening) in some regions after this time [*Wild et al.*, 2005; *Pinker et al.*, 2005].

[3] Though global studies of this climatic parameter are important to assess the spatial representativeness of this phenomenon, research performed at smaller spatial and time scales, i.e., seasonally, has allowed additional knowledge to be gained including a closer look at its underlying mechanisms [*Pozo-Vázquez et al.*, 2004; *Sanchez-Lorenzo et al.*, 2008; *Stjern et al.*, 2009; *Chiacchio and Wild*, 2010; *Chiacchio et al.*, 2010]. Largely contributing to these decadal variations in DSW are changes in cloud cover and aerosols with the latter pointing toward an anthropogenic cause when clear-sky is considered [*Wild*, 2009] and when satellite-derived aerosol data are used [*Cermak et al.*, 2010]. With related studies focused on a more regional spatial scale like Europe [*Norris and Wild*, 2007; *Ruckstuhl et al.*, 2008; *Sanchez-Lorenzo et al.*, 2008; *Stjern et al.*, 2009; *Chiacchio and Wild*, 2010], it has been suggested that anthropogenic aerosols govern the DSW mainly during spring and summer while the North Atlantic Oscillation (NAO) and its associated cloud cover mainly drives DSW in winter and autumn [*Chiacchio et al.*, 2011].

[1]Institute for Atmospheric and Climate Science ETH, Zurich, Switzerland.
[2]Earth System Physics, Abdus Salam International Centre for Theoretical Physics, Trieste, Italy.
[3]School of Engineering, Computing and Mathematics, University of Exeter, Exeter, UK.

Corresponding author: M. Chiacchio, Earth System Physics, Abdus Salam International Centre for Theoretical Physics, Strada Costiera 11, IT-34151 Trieste, Italy. (mchiacch@ictp.it)

0148-0227/12/2012JD017620

[4] Though the role of aerosols on DSW is important to assess both from a natural and an anthropogenic influence [*Hatzianastassiou et al.*, 2007], considering only the effects from clouds and atmospheric circulation remain complex and thus, should be studied in more detail. A deeper understanding of the relationship between the two latter natural climate components with DSW is critical to allow a better linkage to be made in the future with temperature and precipitation variations where as much as 75% in many regions of the world are controlled by extratropical circulation modes of variability [*Quadrelli and Wallace*, 2004; *Rauthe and Paeth*, 2004; *Paeth and Pollinger*, 2010]. The NAO and temperature variability relationship, for example, is found to be more complex and nonlinear in southern Europe when compared to the link between NAO and northern European temperatures [*Castro-Díez et al.*, 2002]. *Castro-Díez et al.* [2002] also found that southern European temperatures driven by the NAO are mainly due to the phase and position of the action center of the NAO. The NAO is also largely responsible for cloudiness variability in southern Europe and the Mediterranean [*Lolis*, 2009] as well as partly contributing to changes in precipitation over the North Atlantic Ocean [*Mariotti and Arkin*, 2006]. Thus, any changes in the low-frequency variability of the NAO, i.e., both from internal natural variability [*Semenov et al.*, 2008] and possible external radiative forcing caused by anthropogenic climate change [*Osborn et al.*, 1999; *Paeth et al.*, 1999; *Ulbrich and Christoph*, 1999; *Visbeck et al.*, 2001; *Bojariu and Gimeno*, 2003; *Gillett et al.*, 2003; *Stephenson et al.*, 2006; *Deser and Phillips*, 2009; *Paeth and Pollinger*, 2010; *Chiacchio et al.*, 2011], could have large impacts on climate [*Hurrell et al.*, 2006]. Because a connection is found between the NAO and extreme events in many climate parameters including temperature and precipitation in the Northern Hemisphere [*Thompson and Wallace*, 2001; *Gillett et al.*, 2003], there is the possibility then that the NAO even under forcing could be related to, for example, an increase in the number and the intensification of heat waves in the Mediterranean [*Kuglitsch et al.*, 2010], an increase in summer temperature variability [*Xoplaki et al.*, 2003], possibly accounting for summer European heatwaves [*Schär et al.*, 2004], and an increase in extreme temperatures in the western Mediterranean [*Hertig et al.*, 2010]. Knowledge of the interactions between these circulation patterns and DSW as well as cloud cover and DSW is crucial in order to determine whether a link exists between these parameters and extreme events in the Mediterranean, for example. More attention should be given to this region because it is also a climate change "hot spot" in the 21st century [*Giorgi*, 2006] making it one of the most sensitive regions to climate change in the world.

[5] Though the NAO has been studied before including its role on DSW [*Pozo-Vázquez et al.*, 2004; *Chiacchio and Wild*, 2010], we perform this analysis with more detailed statistical techniques using generalized linear models (GLMs) and with other less known but important circulation patterns including the Mediterranean Oscillation (MO) and the North Sea Caspian Pattern (NCP) in addition to cloud cover. The interrelationship between these three circulations patterns in the European region in addition to its link with the DSW and cloud cover has not been studied before. Our approach provides new knowledge on the identification of the effects of cloud cover and climatological low-frequency processes in modulating the variability of the DSW and also allows us to assess the relative magnitude of their influence.

2. Data Sets and Methodology

2.1. Downward Surface Solar Radiation

[6] The data used for the DSW were obtained from the Global Balance Energy Archive (GEBA) which is currently maintained at the Swiss Federal Institute of Technology (ETH) in Zurich, Switzerland. Updates have been made to the database as recent as 2007 when major revisions were undertaken. Also, there are station histories available in order to identify the instruments that have recorded the measurements including any changes in their instrumentation as well as quality assessment procedures that flag the data so that errors can be detected. Five quality-control procedures have been applied to the data with a random error of measurements of about 5% for the monthly mean and about 2% for the annual mean [*Gilgen and Ohmura*, 1999]. This database has been used in this paper because it possesses the most complete coverage both spatially and temporally for DSW observations over Europe.

[7] We used GEBA measurements of DSW to evaluate its relationship to cloud cover and atmospheric circulation patterns. Time series of seasonal means of DSW from GEBA have been constructed for the period 1971–1996 with a total of 44 stations listed in Table 1 by their names and coordinates. Figure 1 shows the geographical distribution of these DSW stations which have been numbered corresponding to those from the table from west to east. This period was chosen so that it would coincide with available cloud cover data that is available only at this time. It is also a time span that contains a large number of stations requiring that no more than 3 months were missing within any year and that no more than 4 years were missing in a particular stations' time series.

2.2. Cloud Cover Data

[8] Total cloud cover measurements were used in this study and were extracted from a cloud climatology data set from land stations over Europe for the available period 1971–1996 on a monthly and seasonal basis from the Carbon Dioxide Information Analysis Center (CDIAC) located under the United States Department of Energy at the Oak Ridge National Laboratory. Other data sets at this center include gridded cloud climatology from surface observations over land from 1971 to 1996 and over ocean covering the period 1954–1997. The data were originally taken from surface synoptic weather reports every 3 h from over 5000 land weather stations worldwide. From these reports, averages of total cloud cover as well as those from 9 different cloud types were computed [*Hahn and Warren*, 2003]. In addition, the frequency of occurrence of clouds and the clear-sky frequency are provided. In our study we co-located the monthly averaged total cloud cover from 44 individual stations within Europe that were within 1° latitude × 1° longitude to the DSW measurements from GEBA (Figure 1). Table 1 shows a list of all 44 cloud cover stations used with their coordinates and names according to their corresponding nearest DSW station. A more in-depth description of the method that was used to compute the averaged cloud cover used can be seen in

Table 1. List of the Downward Surface Shortwave Radiation (DSW) Stations and Their Coordinates With the Coordinates of the Corresponding Nearest Cloud Cover Station

	DSW Station			Cloud Cover Station	
Station Number	Station	Longitude (deg)	Latitude (deg)	Longitude (deg)	Latitude (deg)
1	Valentia	−10.25	51.9	−10.25	51.93
2	Kilkenny	−7.27	52.6	−8.25	51.8
3	Aldergrove Airpt.	−6.22	54.6	−5.7	55.43
4	Aberporth	−4.57	52.1	−4.8	52.75
5	Eskdalemuir	−3.2	55.3	−3.35	55.95
6	Lerwick	−1.19	60.1	−0.88	60.85
7	Bracknell	−0.79	51.3	−0.48	52.22
8	London, Weather C.	−0.12	51.5	0.05	50.78
9	Limoges	1.28	45.8	0.32	46.58
10	Millau	3.01	44.1	3.02	44.12
11	Uccle	4.35	50.8	3.6	51.45
12	DeBilt	5.18	52.1	4.42	52.18
13	Bergen	5.31	60.4	4.72	60.75
14	St. Hubert	5.4	50	5.78	50.92
15	Wageningen	5.65	51.9	4.77	52.3
16	Nancy-Essey	6.21	48.6	6.13	49.08
17	Trier	6.66	49.7	5.92	50.48
18	Nice	7.2	43.6	6.5	44.57
19	Locarno-Monti	8.78	46.1	8.73	45.62
20	Ajaccio	8.8	41.9	8.68	42.52
21	Wuerzburg	9.96	49.7	9.95	50.5
22	Hamburg	10.11	53.6	9.55	54.53
23	Braunschweig	10.45	52.3	10.62	51.8
24	Weihenstephan	11.7	48.4	10.97	49.03
25	Vigna di Valle	12.21	42	12.98	42.47
26	Taastrup/Copenhagen	12.3	55.6	12.45	56.3
27	Klagenfurt	14.33	46.6	13.65	47.1
28	Messina	15.55	38.2	16.25	38.9
29	Kolobrzeg	15.58	54.1	15.58	54.18
30	Amendola	15.71	41.5	15.72	41.53
31	Hradec-Kralove	15.85	50.2	14.95	51.17
32	Sljeme-Puntijarka	15.96	45.9	15.9	46.87
33	Wien, Hohe Warte	16.36	48.2	15.95	48.77
34	Brindisi	17.95	40.6	17.95	40.65
35	Stockholm	17.95	59.3	17.6	59.88
36	Budapest	19.18	47.4	18.2	47.87
37	Zakopane	19.96	49.2	19.15	48.63
38	Belsk	20.78	51.8	20.97	52.17
39	Warszawa	20.98	52.2	20.35	53.1
40	Lulea	22.13	65.5	21.63	66.38
41	Jokioinen	23.5	60.8	23.58	61.42
42	Sodankyla	26.65	67.3	26.65	67.37
43	Kiev	30.45	50.4	30.23	51.28
44	Odessa	30.63	46.4	30.63	46.48

Warren and Hahn [2002]. In this latter study they give a detailed description of the strict quality control measures and processing procedures that are applied to the cloud observations, which improves the accuracy of these observations for climate research.

2.3. Atmospheric Circulation Patterns

2.3.1. North Atlantic Oscillation Index

[9] The NAO index (NAOI) used in the analysis represents the monthly averaged normalized pressure difference between the station of Gibraltar and South-West Iceland obtained from the Climate Research Unit (CRU) at the University of East Anglia in Norwich, United Kingdom [*Jones et al.*, 1997]. By inspecting the NAO index, decadal changes and trends can be seen which illustrates the variability of this dominant mode of variability. This pattern influences the climate from the eastern part of the United States to Siberia and from the Arctic to the subtropical Atlantic primarily during winter [*Hurrell et al.*, 2003]. The NAO is an important climate pattern governing the structure and pattern of surface temperature and precipitation plus many other socio-economic factors [*Hurrell*, 1995]. Thus, understanding the causes of its variability including its phase change through either internal or external mechanisms is essential for its prediction.

2.3.2. Mediterranean Oscillation Index

[10] The MO index (MOI) is a time series of 3-monthly averages obtained from CRU and represents the normalized pressure difference between Algiers, Algeria and Cairo, Egypt [*Conte et al.*, 1989]. It is one of the most important regional low-frequency patterns over the Mediterranean with a low pressure system (negative phase) linked to strong cyclogenesis over the western part and high pressure system during its positive phase [*Suselj and Bergant*, 2006]. Studies have found a stronger relationship between MO and the Mediterranean climate than between NAO and the Mediterranean climate [e.g., *Conte et al.*, 1989; *Suselj and Bergant*,

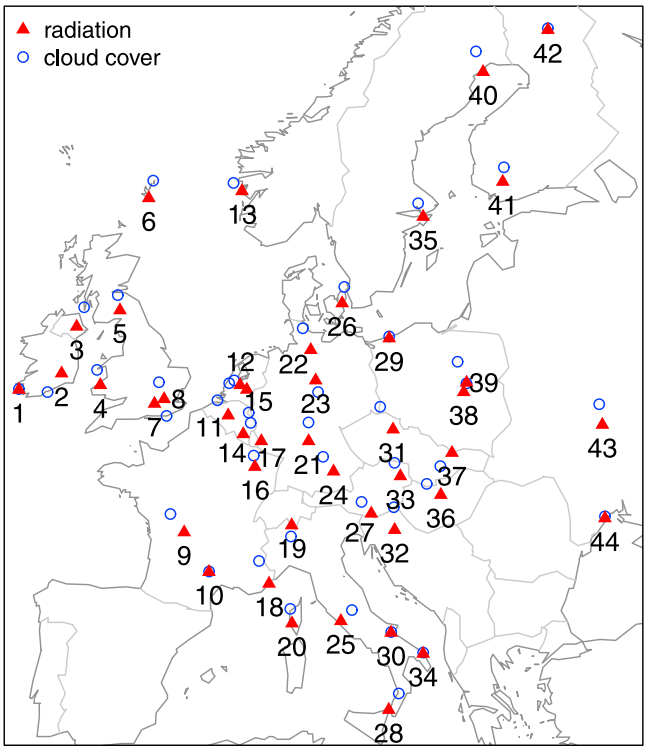

Figure 1. Location of measurement stations of downward surface shortwave radiation (red filled triangles) and cloud cover (open blue circles).

2006]. Thus, in this region, MOI better describes its impact on temperature and precipitation, for example.

2.3.3. North Sea Caspian Pattern Index

[11] The NCP index (NCPI) was obtained from CRU and represents the geopotential height differences between the eastern and western poles of the NCP. The NCP is basically an upper level atmospheric teleconnection pattern between the North Sea and the Caspian Sea at the 500 hPa geopotential level and mainly affects the climate in the eastern Mediterranean [*Kutiel and Benaroch*, 2002]. As found in *Kutiel and Benaroch* [2002], the negative phase of the NCP is characterized by an increased southwesterly anomaly circulation toward the Balkans and western Turkey with above-average temperatures and below-average precipitation while the positive phase shows opposite climatic patterns with an increased northeasterly anomaly circulation toward the Balkans.

2.4. Generalized Linear Models

[12] From our analysis we focused on seasonal timescales and therefore it was restricted to 3-monthly average values of DSW and cloud cover in the usual winter (DJF), spring (MAM), summer (JJA), and autumn (SON) seasons. Denoted by Y^j and C^k, representing the time series of the seasonal DSW at station j and seasonal cloud cover at station k, respectively:

$$Y^j = \left(Y^j_{1971,DJF}, Y^j_{1971,MAM}, Y^j_{1971,JJA}, \ldots, Y^j_{1996,MAM}, Y^j_{1996,JJA}, Y^j_{1996,SON}\right),$$

$$C^k = \left(C^k_{1971,DJF}, C^k_{1971,MAM}, C^k_{1971,JJA}, \ldots, C^k_{1996,MAM}, C^k_{1996,JJA}, C^k_{1996,SON}\right).$$

[13] The index j ranged from 1 to the number $N_{DSW} = 44$ of DSW measurement stations. Similarly, k ranged between 1 and the number $N_{CC} = 44$ of total cloud cover measurement stations. In general, the cloud cover measurement stations did not coincide with the DSW stations (see Figure 1), hence it made sense to consider distinct indices j and k. We studied the physical influence of cloud cover on DSW by means of two GLMs where cloud cover and seasonality both acted as covariates to explain the temporal variability of DSW. The first model is a multiple linear regression:

$$\begin{aligned} Y^j \sim \text{Normal}(\mu,\sigma), \mu = {} & \beta_0 + \beta_1 C^k + \beta_2 \text{DJF} + \beta_3 \text{MAM} \\ & + \beta_4 \text{JJA} + \beta_5 \text{SON} + \beta_6 \text{Time} \\ & + \beta_7 \text{TimeDJF} + \beta_8\ \text{TimeMAM} \\ & + \beta_9 \text{TimeJJA} + \beta_{10} \text{TimeSON} \end{aligned} \quad (1)$$

where Normal(μ, σ) denotes a Gaussian random variable with mean μ and standard deviation σ. The mean response μ is referred to as the *systematic component* of the model. The strong seasonal variations in DSW were taken into account by four indicator variables, DJF, MAM, JJA, and SON which were set to 1 in the corresponding season of each year and 0 otherwise. Long-term temporal trends were taken into account by a variable Time increasing linearly from 0 to 1 with time (as identified by the progressive number of the seasons). We considered interaction terms between this variable and the four seasons to allow for different (linear) trends in different seasons. We also considered a Gamma GLM with inverse link:

$$\begin{aligned} Y^j \sim \text{gamma}(\theta,\nu), 1/\mu = {} & \gamma_0 + \gamma_1 C^k + \gamma_2 \text{DJF} + \gamma_3 \text{MAM} \\ & + \gamma_4 \text{JJA} + \gamma_5 \text{SON} + \gamma_6 \text{Time} \\ & + \gamma_7 \text{TimeDJF} + \gamma_8\ \text{TimeMAM} \\ & + \gamma_9 \text{TimeJJA} + \gamma_{10} \text{TimeSON}. \end{aligned} \quad (2)$$

[14] Here gamma(θ, ν) denotes a gamma-distributed random variable with mean $\mu = \theta\nu$, scale parameter $\theta > 0$ and shape parameter $\nu > 0$, having probability density

$$f(x;\theta,\nu) = x^{(\nu-1)} e^{(-x/\theta)} / \theta^k \Gamma(\nu), \text{ with } x > 0.$$

[15] The reason for using the two different models (1) and (2) (equations (1) and (2)) is that they capture different behaviors, since they differ in both the systematic component, which is linear in (1) and nonlinear in (2), and in the random variability around the systematic component, which is Gaussian (symmetric) in (1) and Gamma (asymmetric or skewed) in (2). We shall return on this point when discussing the performances of the two models in section 3.1.

2.5. Remark

[16] The main purpose of models (1) and (2) was to determine the physical influence of cloud cover at station k on DSW at station j. In general, it can be expected that if the two stations are nearby, then an increase in cloud cover corresponds to a decrease in observed DSW. In the rest of the paper we shall refer to this situation as a "negative effect" of the cloud cover at station k on the DSW at station j. Similarly, we shall speak of a "positive effect" if an increase in cloud cover corresponds to an increase in DSW: such apparently counterintuitive situations do occur, as we shall

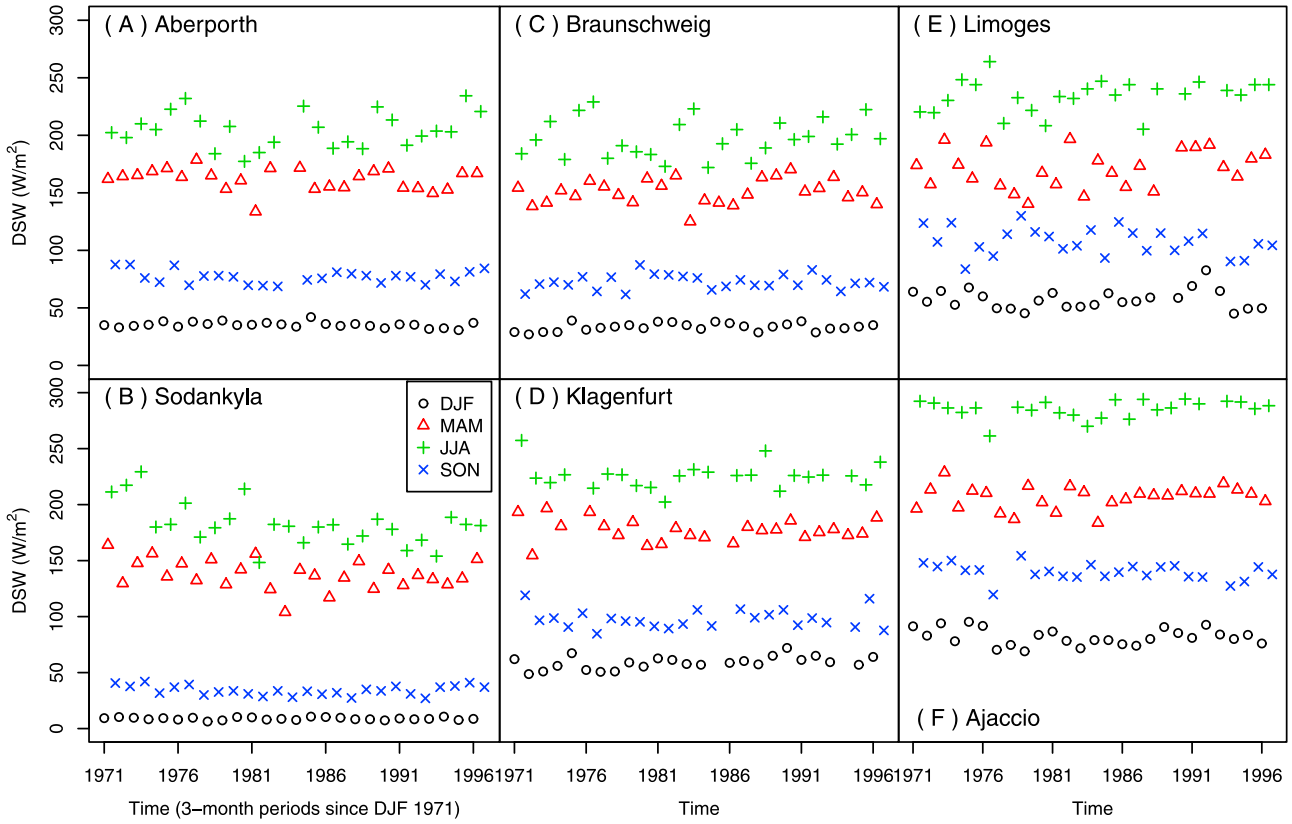

Figure 2. Time series of 3-monthly values of downward surface shortwave radiation at (a) Aberporth, Wales; (b) Sodankyla, Finland; (c) Braunschweig, Germany; (d) Klagenfurt, Austria; (e) Limoges, France; and (f) Ajaccio, Corsica. Values occurring in consecutive 3-monthly periods of December–January–February (DJF), March–April–May (MAM), June–July–August (JJA) and September–October–November (SON) are respectively plotted with circles, triangles, plusses and crosses.

show, for certain cloud cover stations which are far away from the DSW station. For the linear model (1), the physical influence of cloud cover was quantified by the coefficient β_1 in the systematic component: negative values of β_1 imply that cloud cover increase in station k is associated to a decrease of DSW in station j. The situation was exactly the opposite for the Gamma model (2), due to the inverse link in the systematic component: here positive values of the coefficient γ_1 in model (2) imply that cloud cover increase in station k is associated to an increase of DSW in station j. For logical coherence, we shall therefore speak of negative effect of the cloud cover in station k on the DSW in station j if $\beta_1 < 0$ under model (1) and if $\gamma_1 > 0$ under model (2).

[17] Analysis of individual seasons was performed through GLMs where we restricted both the response variable Y and the explanatory variable C to one season (and we therefore did not incorporate indicators for the seasons):

$$Y_S^j \sim \text{Normal}(\mu, \sigma), \mu = \beta_0 + \beta_1 C_S^k + \beta_2 \text{Time}, \quad (3)$$

$$Y_S^j \sim \text{gamma}(\theta, \nu), 1/\mu = \gamma_0 + \gamma_1 C_S^k + \gamma_2 \text{Time}, \quad (4)$$

where S is the season and Time denotes a linear temporal trend term that is a variable ranging linearly from 0 to 1 with the year number. The difference between these two models and models (1) and (2) is that we are now restricting the DSW time series to only one season at a time, as opposed to equations (1) and (2), where all data points are used simultaneously. Therefore, because one-fourth of the data points were used for the latter models, one can expect an overall reduction in the statistical significance of the coefficients β_1 and γ_1 in models (3) and (4) (equations (3) and (4)), respectively as opposed to models (1) and (2), which incorporate data for all seasons.

[18] Lastly, we considered GLMs for the effect of circulation patterns on the DSW:

$$\begin{aligned} Y^j \sim \text{Normal}(\mu, \sigma), \mu = {} & \beta_0 + \beta_1 \text{NAOI} + \beta_2 \text{MOI} + \beta_3 \text{NCPI} \\ & + \beta_4 \text{DJF} + \beta_5 \text{MAM} + \beta_6 \text{JJA} \\ & + \beta_7 \text{SON} + \beta_8 \text{Time} + \beta_9 \text{TimeDJF} \\ & + \beta_{10} \text{TimeMAM} + \beta_{11} \text{TimeJJA} \\ & + \beta_{12} \text{TimeSON} \end{aligned} \quad (5)$$

$$\begin{aligned} Y^j \sim \text{gamma}(\mu, \sigma), 1/\mu = {} & \gamma_0 + \gamma_1 \text{NAOI} + \gamma_2 \text{MOI} \\ & + \gamma_3 \text{NCPI} + \gamma_4 \text{DJF} + \gamma_5 \text{MAM} \\ & + \gamma_6 \text{JJA} + \gamma_7 \text{SON} + \gamma_8 \text{Time} \\ & + \gamma_9 \text{TimeDJF} + \gamma_{10} \text{TimeMAM} \\ & + \gamma_{11} \text{TimeJJA} + \gamma_{12} \text{TimeSON} \end{aligned} \quad (6)$$

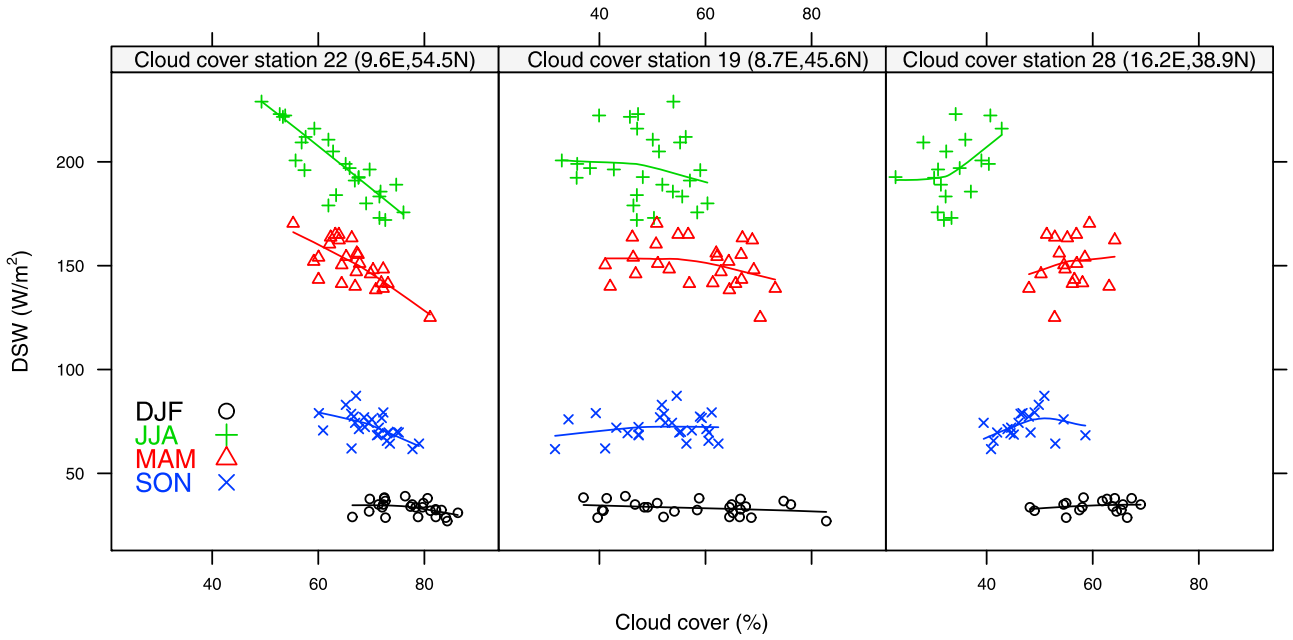

Figure 3. Scatterplot of downward surface shortwave radiation at Braunschweig, Germany (station 23 in Table 1) against cloud cover at three measurement stations: (left) station 22 near Hamburg, Germany; (middle) station 19 near Locarno-Monti, Italy; and (right) station 28 near Messina, Italy with distances of about 138 km to the north, 406 km to the south and 840 km to the south-southwest of Braunschweig, respectively. Values are plotted with different symbols according to the 3-monthly period of occurrence as in Figure 2 and a smoother with a span of 1.1 is superimposed.

where NAOI, MOI, and NCPI are time series of 3-monthly averages. Similarly to what was done for the cloud cover, we also considered models for the individual seasons:

$$Y_S^i \sim \text{Normal}(\mu, \sigma), \mu = \beta_0 + \beta_1 \text{NAOI}_S + \beta_2 \text{MOI}_S + \beta_3 \text{NCPI}_S + \beta_4 \text{Time}, \quad (7)$$

$$Y_S^i \sim \text{gamma}(\theta, \nu), 1/\mu = \gamma_0 + \gamma_1 \text{NAOI}_S + \gamma_2 \text{MOI}_S + \gamma_3 \text{NCPI}_S + \gamma_4 \text{Time}. \quad (8)$$

[19] The coefficients β_i and γ_i of models (1) and (7) (equation (7)), respectively were estimated by the maximum likelihood approach, using the statistical software R (www.r.-project.org) for all numerical computations.

3. Results

3.1. Effect of Cloud Cover on DSW

[20] In this section we studied the effect of the cloud cover on the DSW focusing on spatial and temporal (seasonal) aspects. Because it would be unwieldy to report individual analyses for each of the 44 DSW stations, we selected a subset of six stations exhibiting spatial patterns which were representative of most of the remaining stations (up to a few exceptions). The selected DSW stations were located in Aberporth, Wales; Sodankyla, Finland; Braunschweig, Germany; Klagenfurt, Austria; Limoges, France; and Ajaccio, Corsica. We shall comment below on the analogies of the remaining DSW stations from the six above.

[21] Figures 2a–2f gives detailed insight into the temporal variability of DSW from these stations showing large variations over the seasons as well as over the whole period 1971–1996. What was also evident from this figure was the stronger grouping of DSW between seasons (i.e., DJF with SON and MAM with JJA) for those stations located farther in the north (Figures 2a–2d) while more southerly stations (Figures 2e and 2f) revealed a greater separation in DSW between all seasons. Thus, depending on location the DSW may be influenced by different atmospheric factors. The following results illuminate the seasonal effect of cloud cover on DSW.

[22] By analyzing the relationship between DSW at Braunschweig and cloud cover from three different measurement stations with increasing distance to one another, the effect that distance had on the relationship between cloud cover and DSW could be closely studied (Figure 3). Cloud cover at station 22 (located near Hamburg, Germany with a distance of about 138 km to the north of Braunschweig (Figure 3, left)) showed a strong negative and linear effect on the DSW, especially in spring and summer and less in winter and autumn. With increasing distance of cloud cover to the DSW station, the relationship became increasingly nonlinear for cloud cover station 19 (located near Locarno-Monti, Switzerland (Figure 3, middle)) and 28 (located near Messina, Italy (Figure 3, right)). The effect also became positive for cloud cover station 28. Overall these effects of cloud cover on the DSW were largely pronounced in spring and summer and less in winter and autumn.

[23] To further evaluate the complex relationship as illustrated above between cloud cover and DSW, a Gaussian regression model (equation (1)) and Gamma GLM (equation (2)) were applied to model these results. We first considered the DSW at Braunschweig (10.5E, 52.3N) and cloud cover at a station located slightly southwest (10E, 50.5N) near

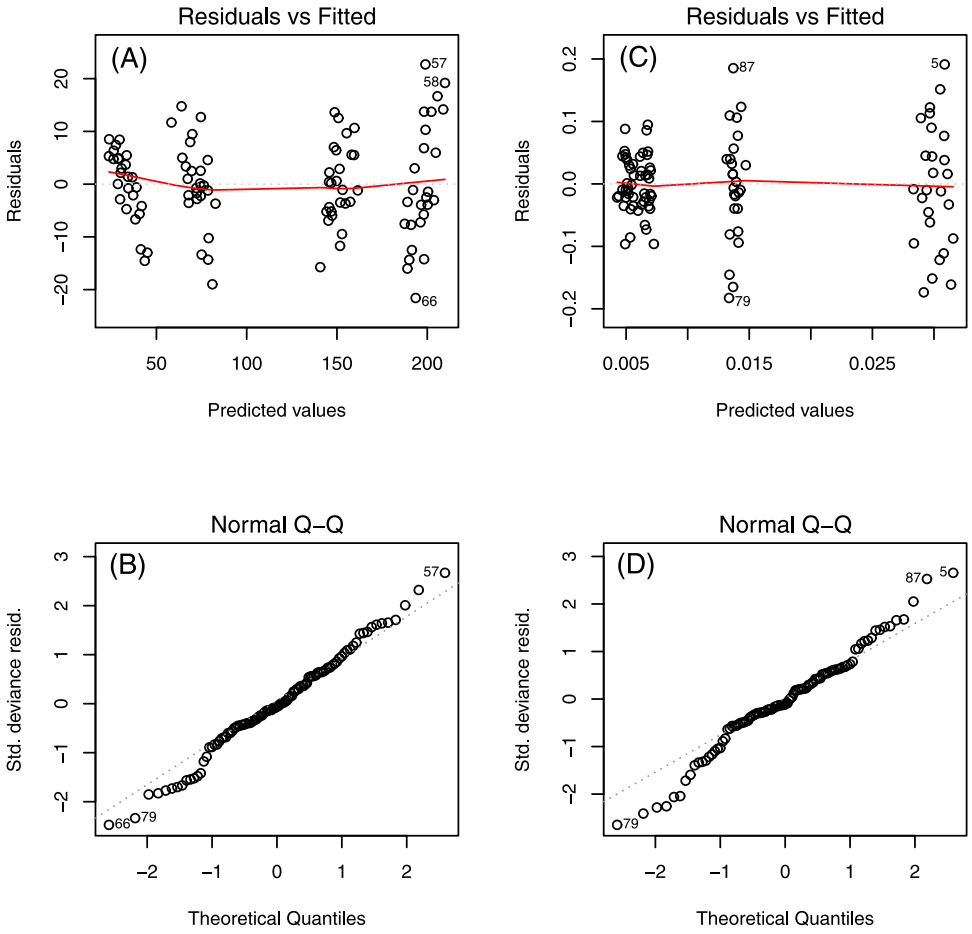

Figure 4. Diagnostic plots (a and b) for the Gaussian regression model of equation (1) and (c and d) for the Gamma generalized linear model of equation (2), for the downward surface shortwave radiation at Braunschweig, Germany (10.5E, 52.3N) versus the cloud cover at a station located at (10E, 50.5N) near Wurzburg, Germany: Figures 4a and 4c show the residuals of the models versus the fitted values; and Figures 4b and 4d are Quantile-Quantile plots of the standardized deviance residuals against the theoretical quantiles of a standard normal distribution.

Wurzburg, Germany. The first step of our analysis was the qualitative graphical inspection of diagnostic plots based on the so-called *deviance residuals* of the model. The deviance is a quantitative measure of discrepancy between model predictions and observed data, see chapter 2 of *McCullagh and Nelder* [1989]. Deviance residuals express the contribution to the total deviance by each individual pair of predicted/observed values. For the linear model in equation (1), the deviance residuals are simply given by the differences between the predicted and the observed values. For the Gamma GLM in equation (2) they have a more complex expression, see section 2.4.3 of *McCullagh and Nelder* [1989].

[24] Graphical inspection of the residual plots allows one to quickly assess the appropriateness of modeling assumptions such as linearity versus nonlinearity and overall model performance. The first type of diagnostic was the plot of residuals against the predicted values (Figures 4a and 4c). Model inadequacy is indicated by the residuals being not centered around zero and/or having changing variance (heteroskedasticity). The second type of diagnostics was the plot of the quantiles of the empirical distribution of the standardized residuals against the quantiles of a standard normal distribution (Figures 4b and 4d): deviation from the diagonal indicates that the distribution assumed for the random part of the model (in our case, Gaussian or Gamma) is not appropriate.

[25] Qualitative graphical inspection of the residual plots (Figure 4c) showed that the Gamma GLM residuals were better centered near zero compared to the Gaussian model. However, the variances were non-constant for all seasons (the seasons are indirectly identified by the four clusters of predicted values on the horizontal axes of Figures 4a and 4c). We recall that, due to the different definition of deviance for the linear versus the Gamma model (see above), deviance residuals for the linear model (Figure 4a) have the same scale as the original data, whereas this does not hold for the Gamma model (Figure 4c). The Gaussian regression model (Figure 4a) revealed a more constant variance across the seasons but the residuals were less centered near zero. As a result, the quantile-quantile (Q-Q) plot of the Gaussian regression model (Figure 4b) showed less deviation from the diagonal, that is a better fit, than the Gamma GLM (Figure 4d), especially in the upper and lower tails of the

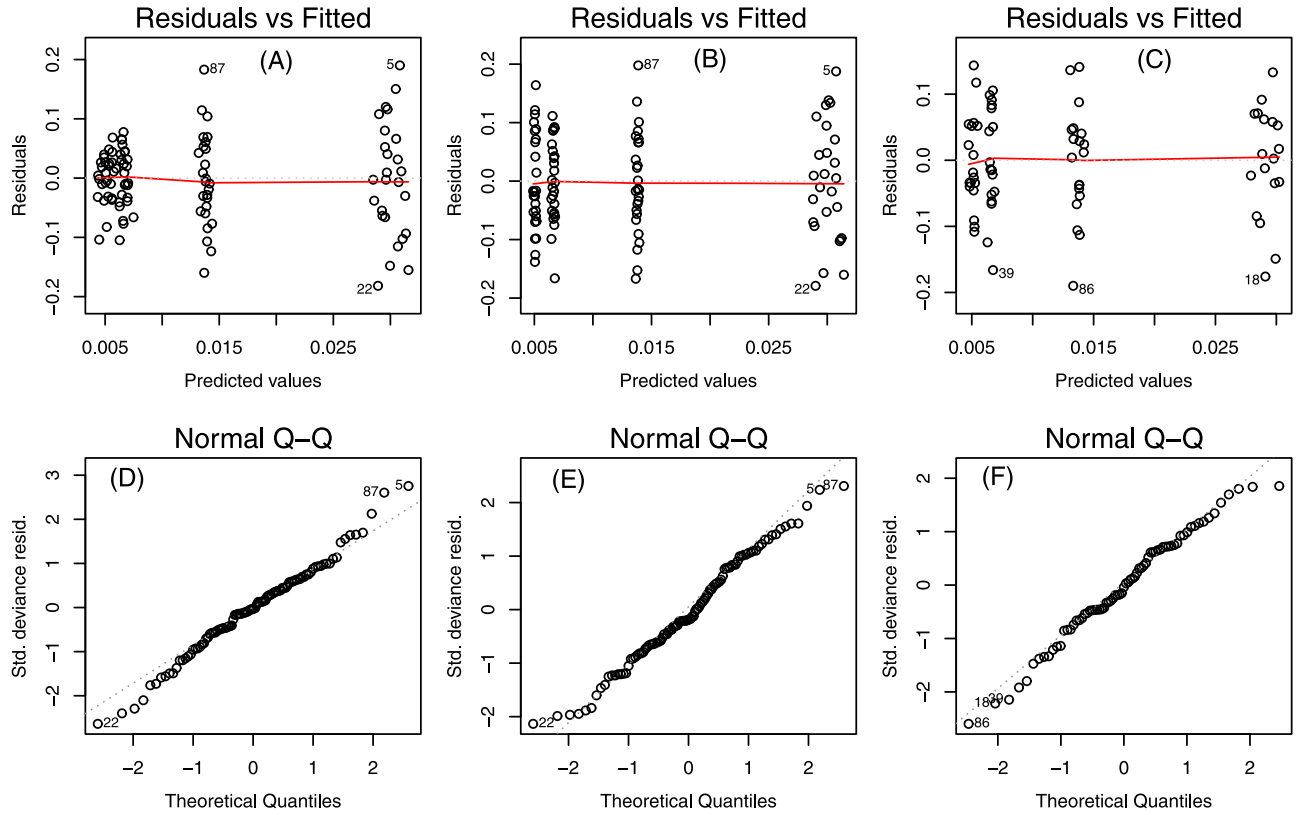

Figure 5. Diagnostic plots as in Figure 4 but for the Gamma generalized linear model fits of the downward surface shortwave radiation at Braunschweig, Germany versus the cloud cover at the stations of Figure 3: (a and d) station 22 near Hamburg, Germany; (b and e) station 19 near Locarno-Monti, Italy; and (c and f) station 28 near Messina, Italy.

distribution. These diagnostic plots illustrated that the Gaussian regression model was more able to capture the residual variability around the predicted values than the Gamma GLM for this particular cloud cover station, which was closest to the DSW station. This agrees with the greater linear dependence of DSW on cloud cover at the nearest cloud cover station as already illustrated by Figure 3.

[26] To examine the performance of the Gamma GLM for cloud cover stations located increasingly farther from the DSW station in Braunschweig, we produced diagnostic plots in Figure 5 similar to those above in Figure 4. We see that with increasing distance of the cloud cover stations, the Gamma GLM overall was still satisfactory to properly model the average signal (systematic component), given the satisfactory alignment on the diagonal in the Q-Q plots (Figures 5d, 5e and 5f). The distribution of the residuals for the farther stations (Figures 5b and 5c) showed more constant variance across the seasons than for the closer station (Figure 5a). This illustrated that the Gamma GLM was able to capture the increasingly nonlinear dependence of DSW on cloud cover for stations located further away, as also illustrated in Figure 3. This change of behavior, from linear to nonlinear, depending on the distance between cloud cover and DSW station, prompted us to examine the results of both the Gaussian and the Gamma GLM to ensure robustness of the detected spatial patterns of dependency of DSW on cloud cover.

[27] In order to study the cloud cover effect on the DSW of the six selected sites, the Gamma GLM was first applied. For each cloud cover station, one independent DSW station measurement was separately fitted in equation (2). As mentioned in section 2.5, positive values of the coefficient γ_1 corresponded to a negative effect of the cloud cover on the DSW. A high degree of spatial coherence was found for the effect of cloud cover on DSW, as represented by the sign of γ_1 (Figure 6). In Figure 6a the DSW station of Aberporth was chosen and showed a statistically significant (at the 95% confidence level) and negative effect of cloud cover in 18 cloud cover stations found south and east of this anchor station including northern France, Germany and Benelux. A neighboring DSW station in Hradec-Kralov, Czech Republic showed similar results as those in Figure 6a (figure not shown). Interestingly, cloud cover from stations in southern Italy, with a total of two that were significant, had a positive effect with DSW at Aberporth.

[28] Features similar to those reported above were also seen for the DSW station of Sodankyla, Braunschweig, and Ajaccio (Figures 6b, 6c, and 6f). It is evident from these results that cloud cover close to the DSW measurement station had a statistically significant negative effect, while cloud cover located farther away from this station overall had a positive effect. The station of Ajaccio, for example, showed the opposite pattern to that of Aberporth, Sodankyla and Braunschweig with a positive but non-significant cloud

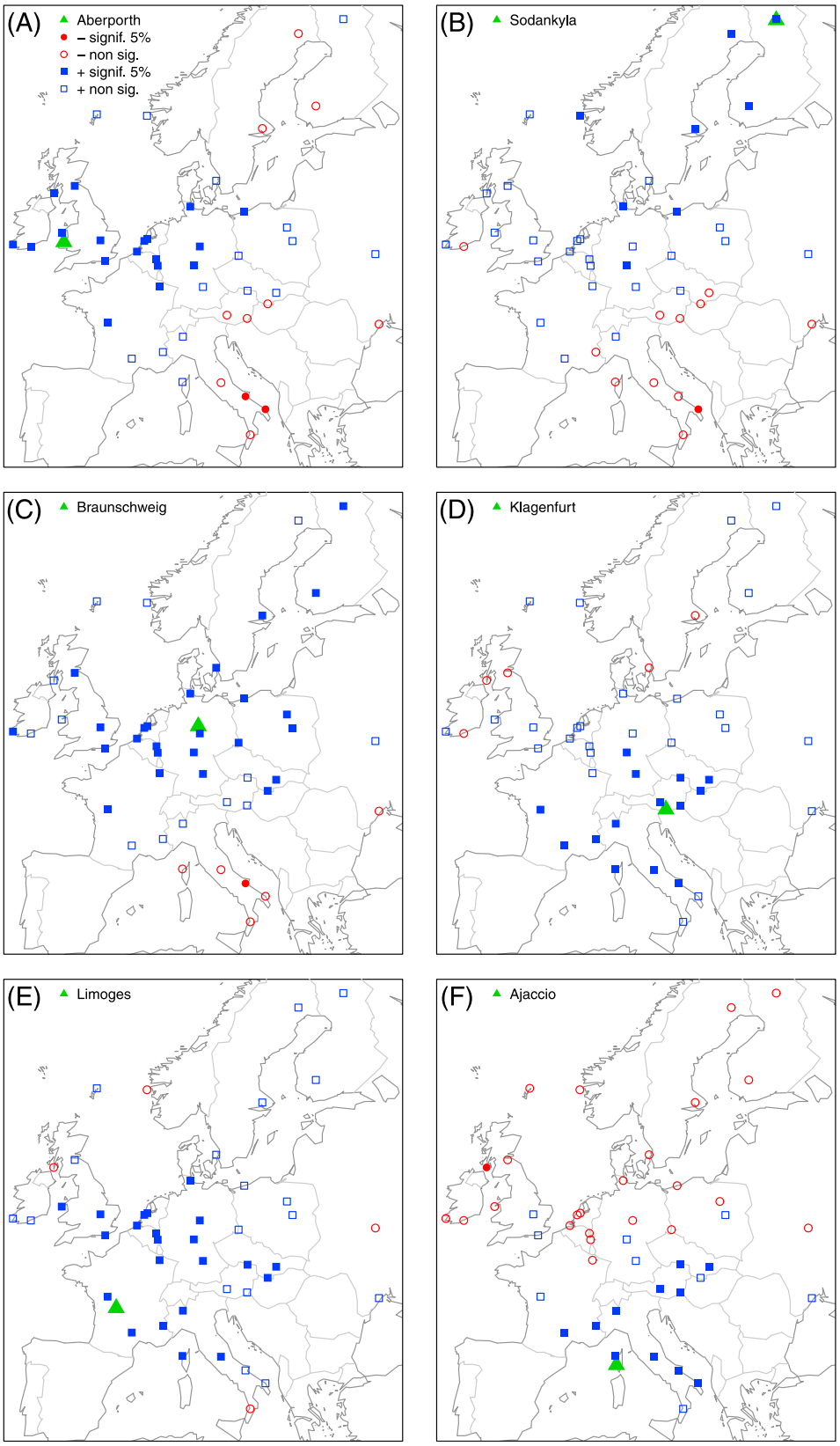

Figure 6. The effects of cloud cover on downward surface shortwave radiation (DSW) under the Gamma generalized linear model of equation (2) at (a) Aberporth, Wales; (b) Sodankyla, Finland; (c) Braunschweig, Germany; (d) Klagenfurt, Austria; (e) Limoges, France; and (f) Ajaccio, Corsica. Cloud cover stations are either represented by red circles (positive effect) or blue squares (negative effect). DSW anchored stations are denoted as green filled triangles.

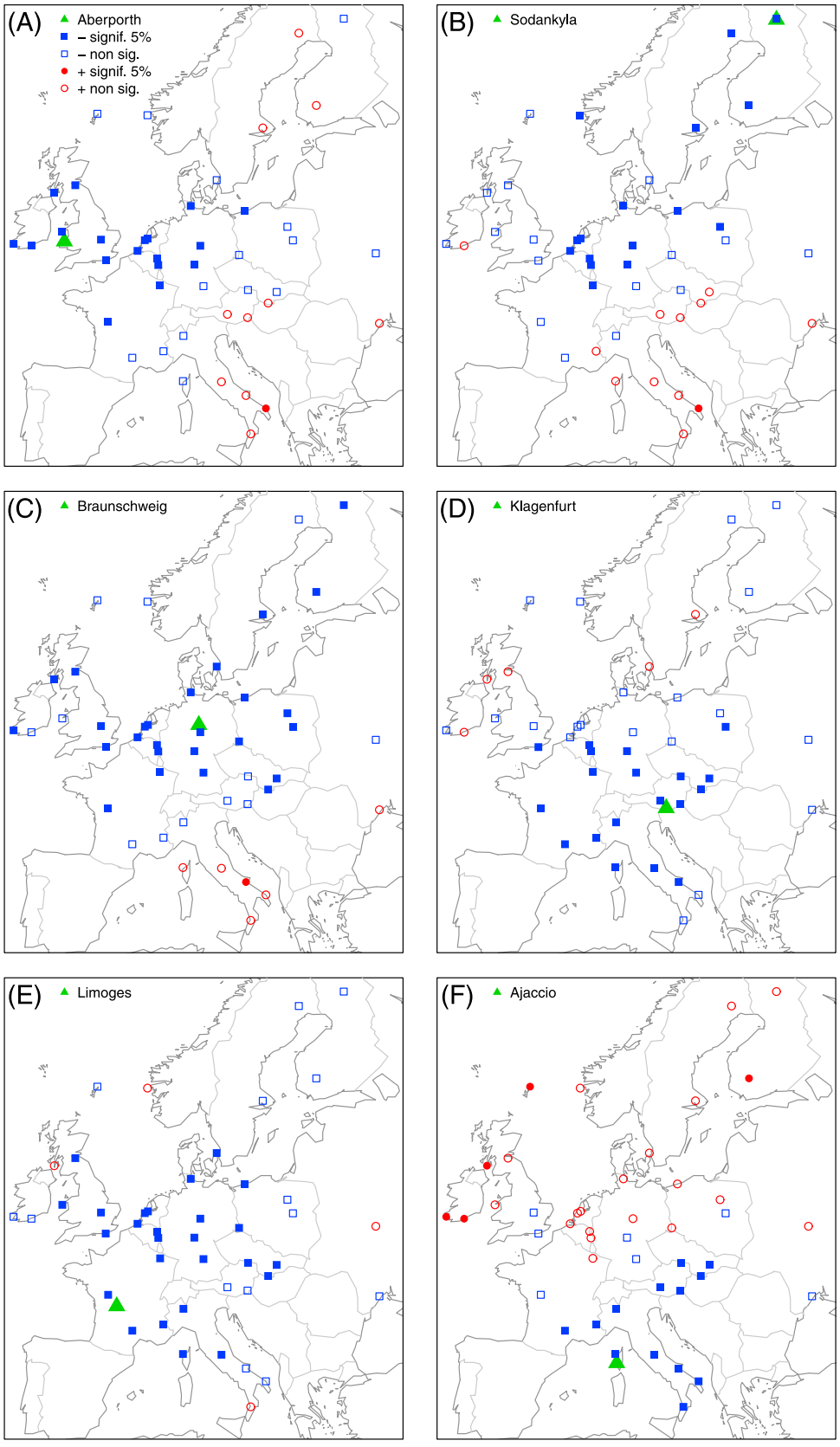

Figure 7. As in Figure 6 but for the Gaussian regression model of equation (1).

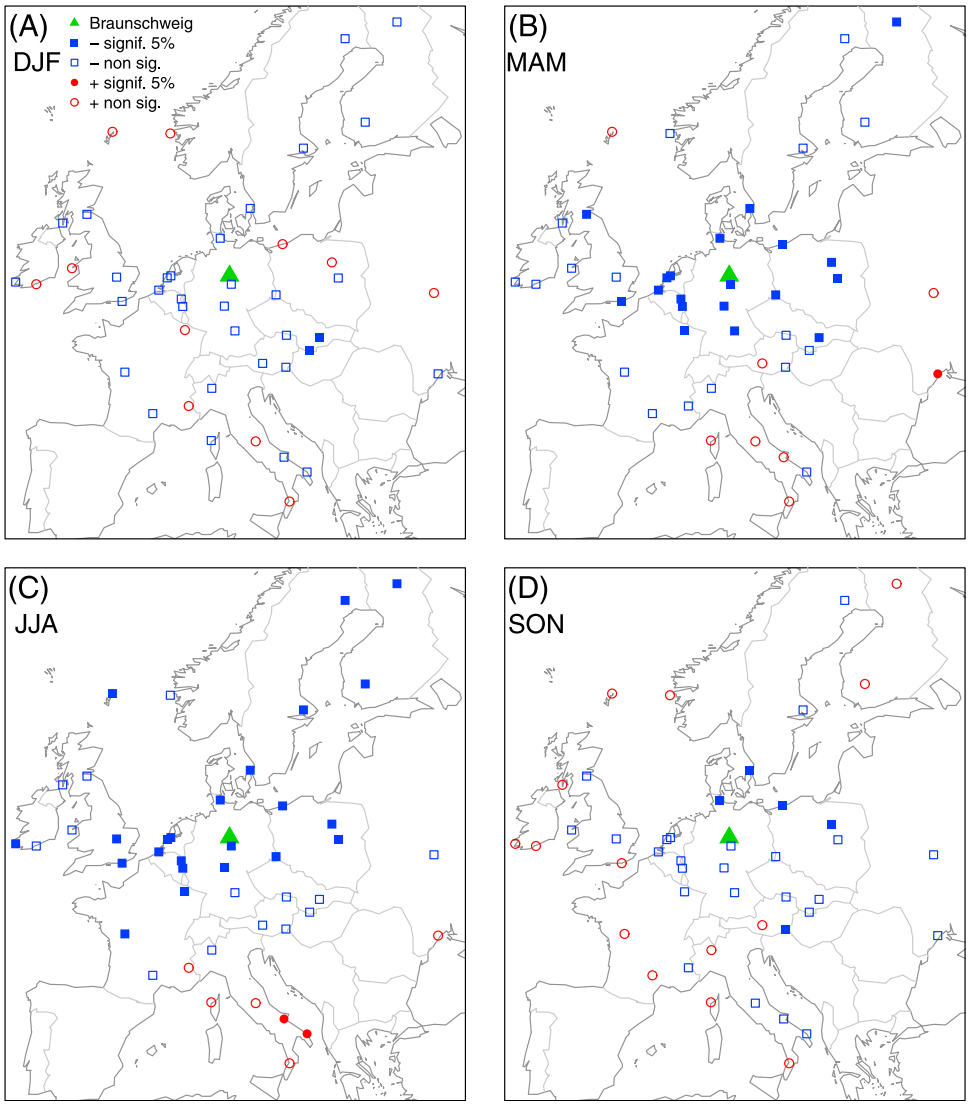

Figure 8. The effects of cloud cover on downward surface shortwave radiation (DSW) under the individual season linear regression model of equation (3) for a DSW selected station located in Braunschweig, Germany: (a) winter (December–January–February, DJF); (b) spring (March–April–May, MAM); (c) summer (June–July–August, JJA); and (d) autumn (September–October–November, SON). Cloud cover stations are either represented by red circles (positive effect) or blue squares (negative effect). DSW anchored stations are denoted as green filled triangles. Significant values at the 5% significance level are either red filled circles or blue filled squares.

cover effect now located in central to the northern part of Europe and a significant (11 stations in total) negative effect closer to the station of Ajaccio. Exception to this main pattern of positive and negative effects was seen in Klagenfurt and Limoges (Figures 6d and 6e), where DSW stations in west-central Europe had an overall negative effect over the whole continent. However, the cloud cover effect was not significant for more remote stations.

[29] The whole analysis on the effect of cloud cover on DSW was also repeated using the Gaussian regression model of equation (1) (Figure 7) using identical anchored DSW stations as in Figure 6. For this model, negative values of β_1 corresponded to a negative effect of the cloud cover on the DSW (see again section 2.5). For logical coherence with Figure 6, we maintained the same color and symbol coding in Figure 7 for the cloud cover stations having negative effects on the DSW, although the sign of β_1 (also reported in the figure legend) was negative under model (1), whereas $\gamma_1 > 0$ for such stations under model (2). These stations showed the same patterns as for the Gamma GLM model, with mainly a negative and statistically significant cloud cover effect near the DSW site and a positive but less significant effect located more remotely (Figures 7a–7c and 7f). The exception to this feature was found for the stations of Klagenfurt and Limoges (Figures 7e and 7f) as before in Figure 6 with an overall negative cloud cover effect throughout Europe. The main difference between results of the Gamma GLM and the Gaussian regression model was the slightly stronger statistical significance shown by the latter model.

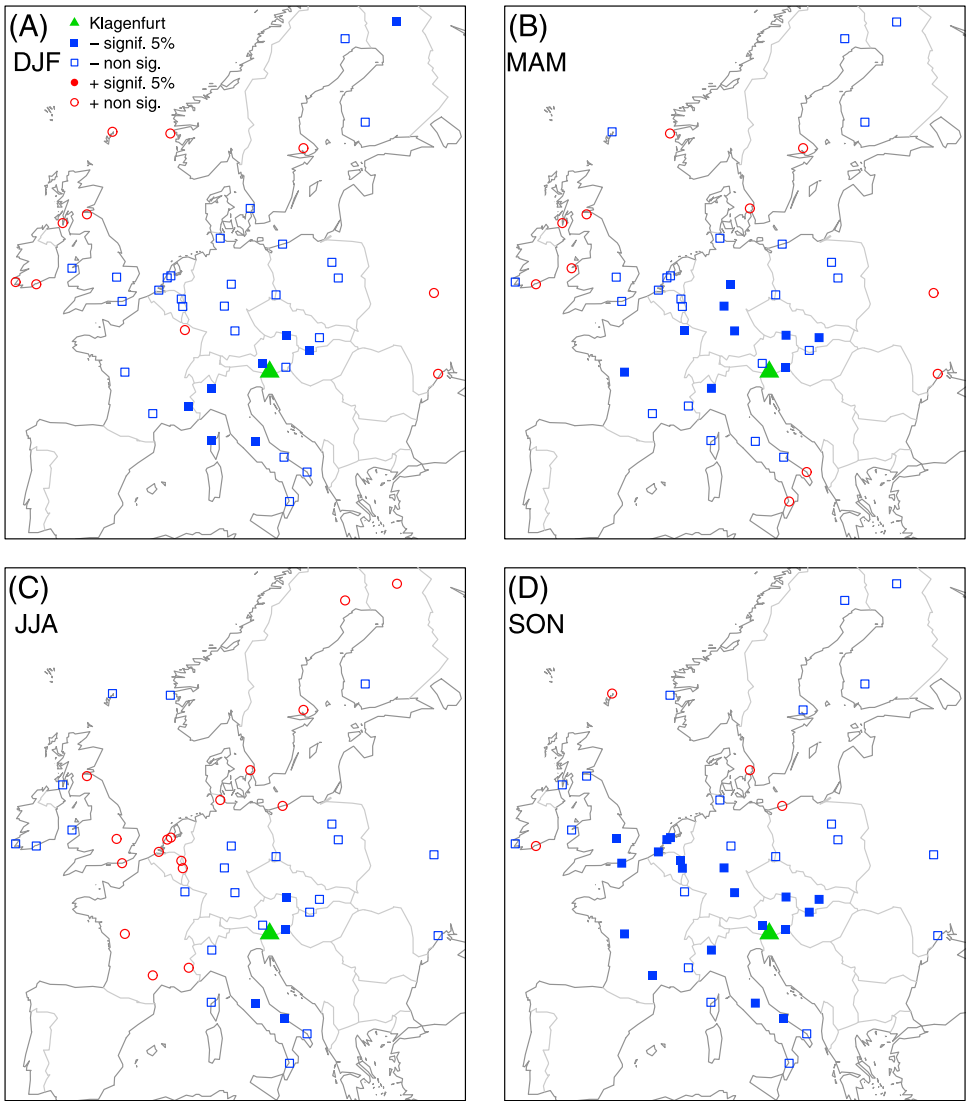

Figure 9. As in Figure 8 but for a downward surface shortwave radiation selected station located in Klagenfurt, Austria: (a) winter (December–January–February, DJF); (b) spring (March–April–May, MAM); (c) summer (June–July–August, JJA); and (d) autumn (September–October–November, SON).

[30] The analyses of Figures 6 and 7 have been carried out for all of the 44 DSW stations and the resulting spatial patterns were very similar to at least one of the six stations shown here. In general, Braunschweig (Figures 6c and 7c) showed a strong negative effect of cloud cover at most stations in continental Europe, which was also typical of DSW stations located in central Europe (e.g., Wageningen, Trier, Wuerzburg, Hamburg, Kolobrzeg, Hradec-Kralove, Wien-Hohe-Warte). This pattern was also similar to that of DSW stations in central France (Limoges, Millau, Nancy-Essey) and the Benelux countries (Uccle, DeBilt, St Hubert). Aberport's pattern was typical of DSW stations located in the British Isles (e.g., Kilkenny, Aldergrove Airport, Eskdalemuir): negative cloud cover effects were more concentrated in central continental Europe (France, Germany, the Benelux countries). DSW stations located in the Scandinavian countries (e.g., Bergen, Stockholm, Lulea, Jokioinen) exhibited a pattern similar to that of Sodankyla: negative effects of cloud cover were mainly located in the northeast of Europe. DSW stations located in southern Europe, either south of the Alps or on the Mediterranean (Nice, Vigna di Valle, Brindisi, Messina) had negative cloud cover effects concentrated near the DSW station. The DSW stations at Kiev and Odessa (not shown) are characterized by spatial patterns that are rather different from those discussed so far with more limited dependence on the cloud cover measured in the rest of Europe.

[31] In order to further investigate the cloud cover effect on DSW according to different seasons, the individual season linear regression model (equation (3)) was used. As the anchored DSW station, we chose the central European site of Braunschweig, which is located in central Germany (Figure 8). In winter (Figure 8a) and autumn (Figure 8d), the negative and positive cloud cover effect on DSW was still evident as reported above but no great statistical significance was found. In spring and summer, on the other hand, many stations revealed statistical significance by as much as

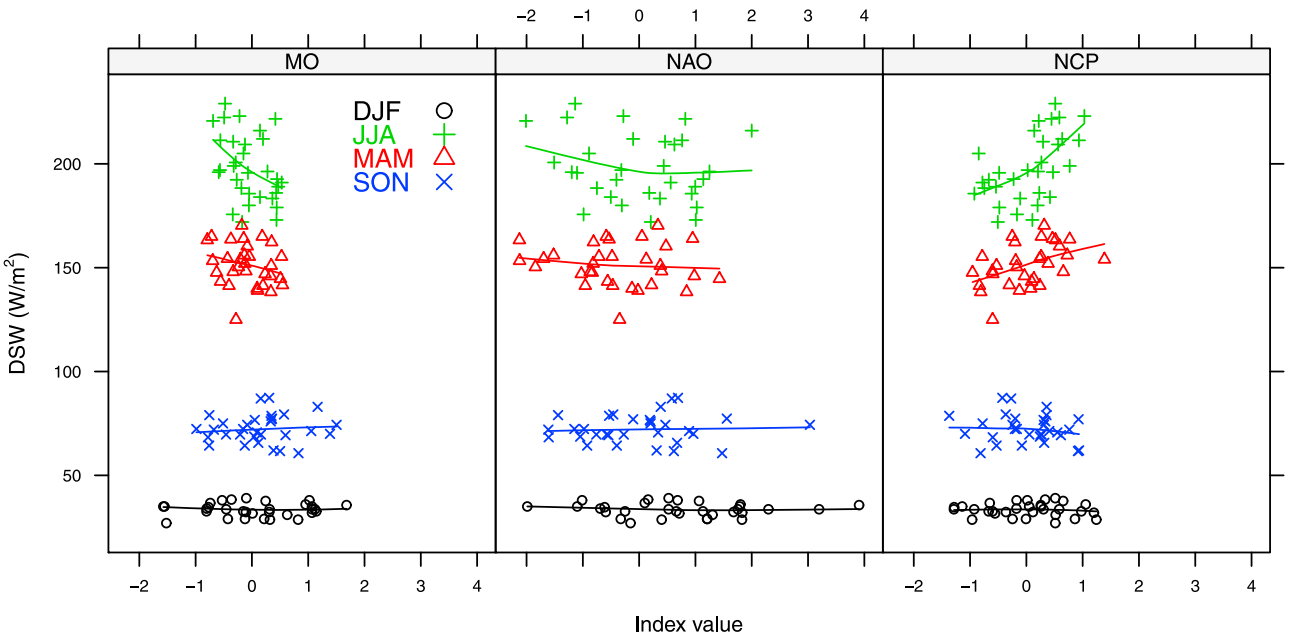

Figure 10. Scatterplot of downward surface shortwave radiation at Braunschweig, Germany against three climate indices: (left) Mediterranean Oscillation (MO); (middle) North Atlantic Oscillation (NAO); and (right) North Sea Caspian Pattern (NCP). Values are plotted with different symbols according to the 3-monthly period of occurrence as in Figure 2 and a smoother with a span of 1.1 is superimposed.

18 stations in spring and 23 in summer located closely around the area of this DSW station. Thus, the cloud cover effect in spring and summer from this DSW station was much stronger than in winter and autumn.

[32] When the anchored DSW station was located further south in Klagenfurt (Figure 9), for example, the cloud cover effect showed statistical significance in all seasons including winter and autumn but less in spring and summer compared to the DSW station of Braunschweig in Figure 8. Winter showed significance with 8 stations located in northern and southern Italy, southern France, Austria, Hungary and Finland (Figure 9a) while in autumn as much as 19 stations were significant and located primarily in central Europe (Figure 9d). Spring and summer (Figures 9b and 9c) revealed a negative cloud cover effect on DSW with 9 stations significant in spring in central Europe and four in summer in southern and central-eastern Europe.

3.2. Effect of Atmospheric Circulation Patterns on DSW

[33] In order to evaluate the atmospheric circulation effect on DSW, a comparison was made between the DSW at Braunschweig and the climate indices of the MO, NAO and NCP (Figure 10). The results generally showed a seasonally varying relationship between DSW and all circulation patterns with nonlinearity mainly in summer and linearity in the other seasons (Figure 10). Specifically, the MO and NCP (Figure 10 (left) and Figure 10 (right), respectively) clearly had opposing effects on the DSW in Braunschweig in spring and summer. In these seasons they showed mainly a negative relationship for the MO and positive for the NCP. The effect of the NAO pattern on the DSW (Figure 10, middle) was not so clear in spring and summer. The overall effect of these circulation patterns on the DSW in winter and autumn were consistent with one another but was less pronounced when compared to the other seasons.

[34] Diagnostic plots, in reference to the effect of circulation patterns on the DSW, were made using the Gaussian regression model (equation (5)) and the Gamma GLM (equation (6)) for the DSW station at Braunschweig (Figure 11). Compared to the Gaussian regression model, the residuals of the Gamma GLM were better centered near zero (Figure 11c) and with a better fit (Figure 11d) but the variances were non-constant across the seasons. The Gaussian regression model, however, revealed a more constant variance for all seasons. Therefore, we used the Gamma GLM to analyze the effect of the circulation patterns on the DSW, while the Gaussian regression model was used when different seasons were considered.

[35] By applying the Gamma GLM in equation (6), the effect of the circulation patterns (NAO, MO and NCP, represented by the coefficients, γ_1, γ_2, and γ_3, respectively), on the DSW was evaluated (Figure 12). The NAO shows mainly a negative effect on the DSW and the statistical significance was not particularly high (Figure 12a). The effect of the MO on DSW (Figure 12b), however, was largely positive in central and southern Europe with statistically significance that was limited to only six stations. Lastly, the NCP showed an extremely clear positive effect with statistical significance throughout central and northeastern Europe (Figure 12c).

[36] The effect of the NAO on the DSW was also analyzed seasonally (Figure 13). The patterns for all seasons essentially showed the sign of the β_1 coefficient in the individual season linear regression model (equation (7)) and included the 3-monthly NAOI. In winter there was clearly a negative effect of the NAO on DSW primarily in northern and central Europe with 9 sites statistically significant in northwestern

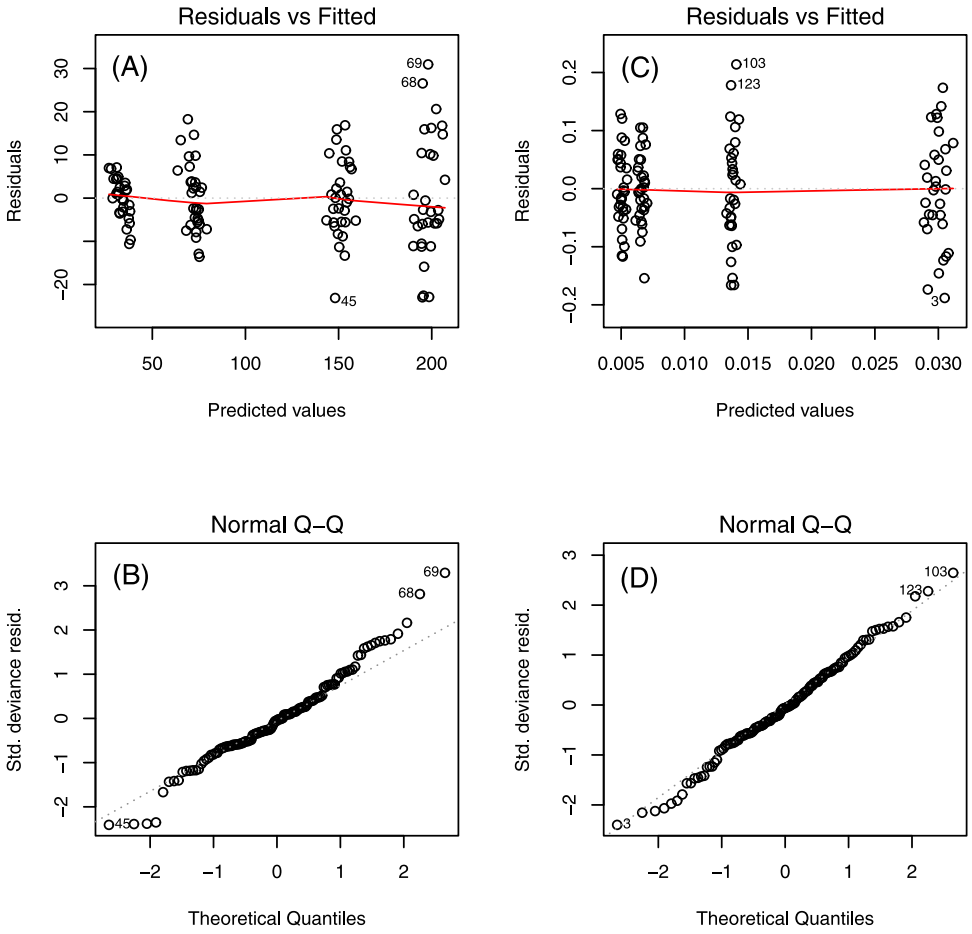

Figure 11. Diagnostic plots (a and b) for the Gaussian regression model of equation (5) and (c and d) for the Gamma generalized linear model of equation (6) for the downward surface shortwave radiation at Braunschweig, Germany versus the circulation pattern indices, MOI, NAOI and NCPI: Figures 11a and 11c show residuals of the models versus the fitted values; and Figures 11b and 11d are Quantile-Quantile plots of the standardized deviance residuals against the theoretical quantiles of a standard normal distribution.

Europe (Figure 13a). In addition, there were four sites showing a positive effect in southern Europe but were non-significant. In spring and summer (Figures 13b and 13c, respectively), however, the NAO did not have the same effect on the DSW with the dipole pattern found above. Instead it showed mainly a negative effect from almost all stations, especially in summer. In autumn (Figure 13d) no significance was found but many sites did show a positive effect located in central-eastern Europe and mainly a negative effect in southern Europe. Clearly this season reflects the opposite pattern seen during winter despite a lack of statistical significance.

[37] The effect of the MO on DSW, which is the sign of the β_2 coefficient in the individual season linear regression model of equation (7), was strongest in winter (Figure 14a). It mainly displayed a positive effect in central to southern Europe with statistical significance in seven sites and four located in the south. Also, the effect of the MO on DSW in autumn was similar to the effect of the NAO on the DSW in winter (Figure 14d), however, none of the DSW station were statistically significant.

[38] The NCP and its effect on the DSW, which is represented by the sign of the β_3 coefficient in the individual season linear regression model of equation (7), overall showed positive effects in spring and summer (Figures 15b and 15c, respectively) with most sites displaying statistical significance in east-central and northern Europe. The NCP clearly had a strong effect on the DSW extending into Scandinavia down to the Ukraine and as wide as the United Kingdom to Eastern Europe. It displayed the largest effect on DSW out of the other two circulation patterns. However, it did not have a strong effect on the DSW in winter and autumn (Figures 15a and 15d, respectively) and no clear-cut spatial patterns were found in these two seasons.

4. Discussion and Conclusion

[39] With a recent focus placed on understanding factors that have governed changes in DSW on a regional and seasonal time scale [e.g., *Pozo-Vázquez et al.*, 2004; *Sanchez-Lorenzo et al.*, 2008; *Stjern et al.*, 2009; *Chiacchio and Wild*, 2010; *Chiacchio et al.*, 2010], this study further investigates and considers a more detailed statistical

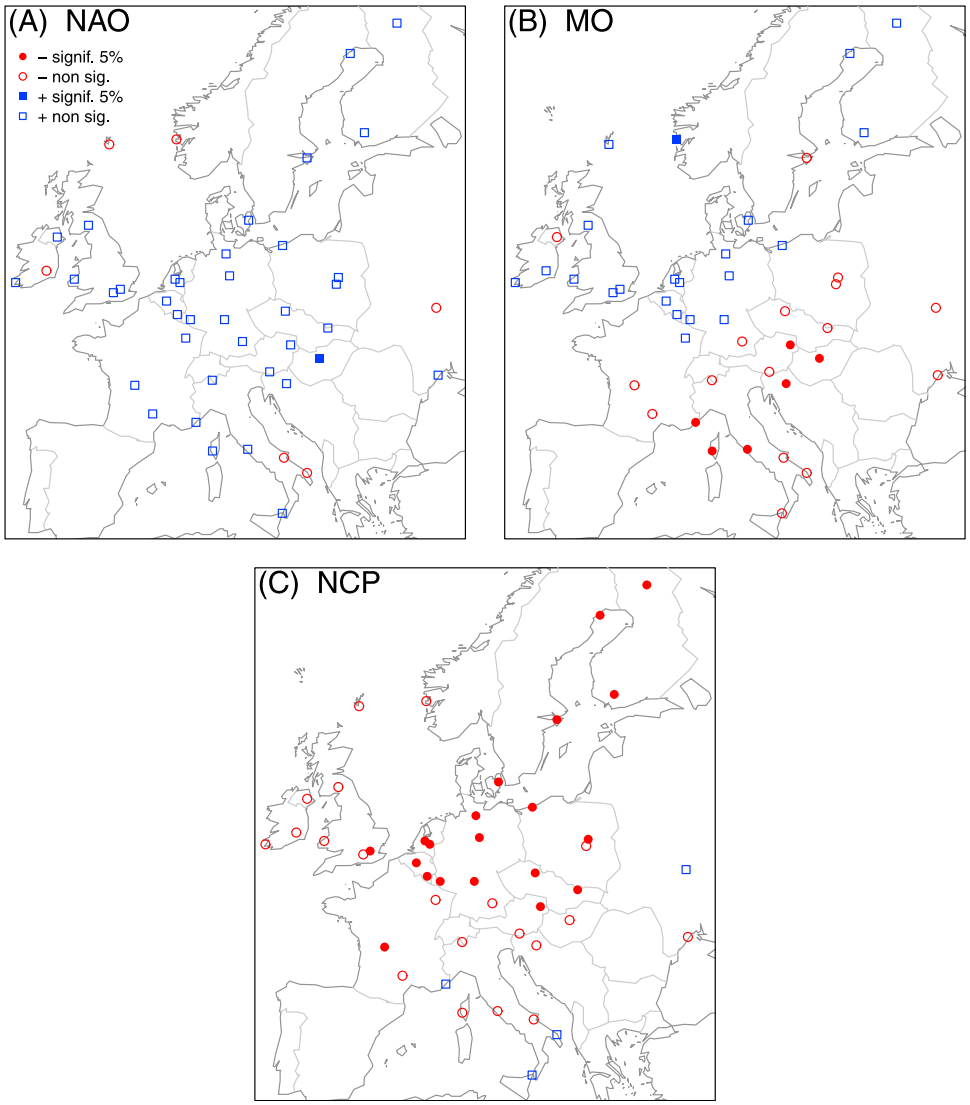

Figure 12. Sign of the coefficients, γ_1, γ_2, and γ_3 from the Gamma generalized linear model equation (6) corresponding to the 3-monthly: (a) North Atlantic Oscillation (NAO); (b) Mediterranean Oscillation (MO); and (c) North Sea Caspian Pattern (NCP) indices, respectively. Red circles represent the positive effect and blue squares the negative effect of these circulation patterns on the downward surface shortwave radiation. Significant values at the 5% significance level are either red filled circles or blue filled squares.

approach using GLM models for the first time to investigate the effects of cloud cover and atmospheric circulation patterns, including the NAO, MO and NCP on DSW in Europe.

[40] The main conclusions from this study revealed the following:

[41] 1. Stations of cloud cover close to the DSW station showed primarily a negative and statistically significant effect while cloud cover stations located remotely showed a positive and non-significant effect. Positive and negative effects of cloud cover on DSW were mainly reported in more northerly or southerly located DSW stations as in Sodanklya and Ajaccio, respectively.

[42] 2. Additional analysis using a basic comparison of DSW anchored in Braunschweig, for example, to increasing distance of cloud cover measured at three different stations revealed a strong and negative linear relationship for those cloud cover stations closer to the DSW site while those farther from the DSW site showed nonlinear and an overall positive relationship (Figure 3).

[43] 3. DSW stations located in west-central Europe (e.g., Klagenfurt and Limoges in Figures 6d, 6e, 7d and 7e), showed an even greater spatial dependence with the negative effect of cloud cover evident throughout Europe but with statistical significance limited to closely located stations of cloud cover.

[44] The latter result suggests that cloud cover stations are associated with synoptic-scale cloud structures and is in line with *Gjertsen* [1997] where a large and extensive low pressure system can be found in central Europe being continuously formed by the Icelandic low. The movement of this cyclone could often be blocked when a high pressure ridge forms due to the Siberian cold high over central Europe. This situation would lead to an increase in cloud cover and large-scale structure in this region. Additionally, this would

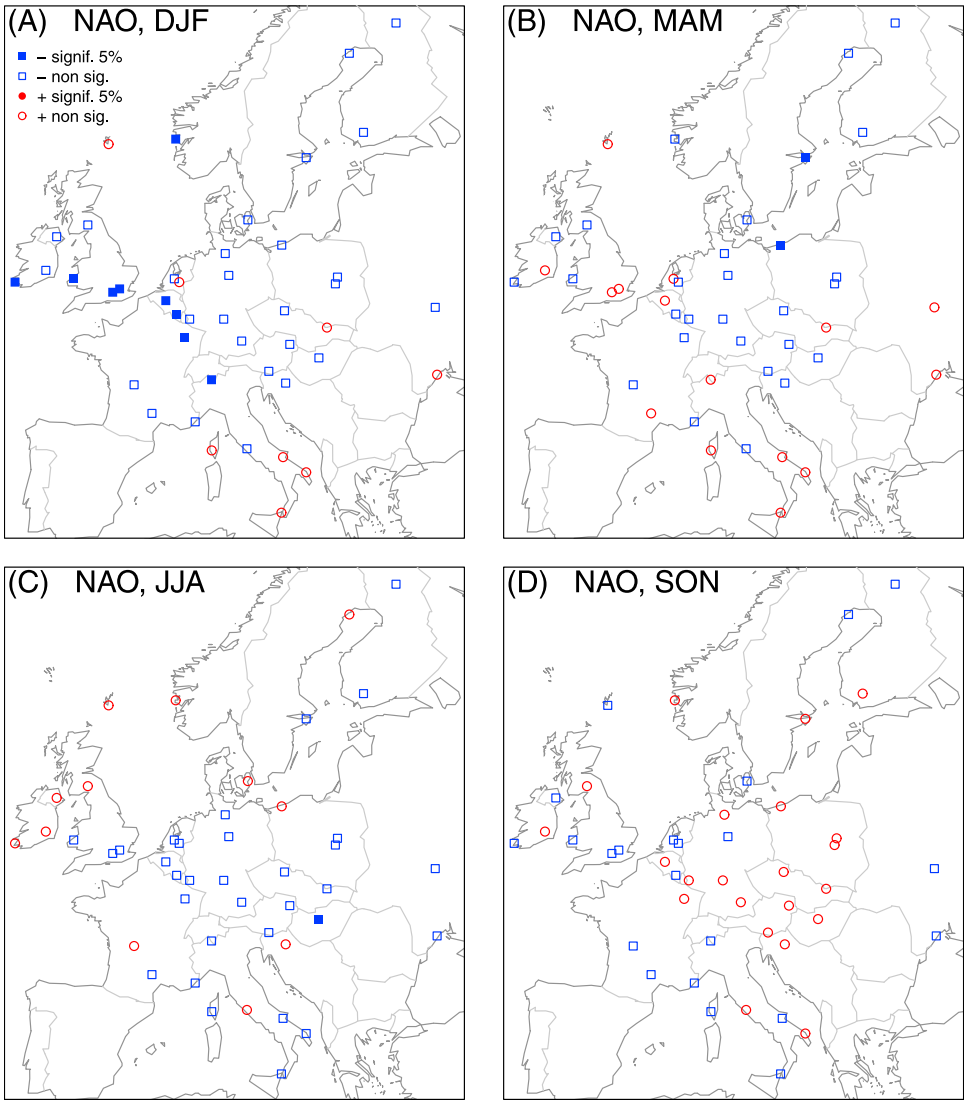

Figure 13. Sign of the β_1 coefficient corresponding to the 3-monthly North Atlantic Oscillation (NAO) index in the individual season linear regression model (equation (7)) for (a) winter (December–January–February, DJF); (b) spring (March–April–May, MAM); (c) summer (June–July–August, JJA); and (d) autumn (September–October–November, SON). Red circles represent the positive effect and blue squares the negative effect of these circulation patterns on the downward surface shortwave radiation. Significant values at the 5% significance level are either red filled circles or blue filled squares.

also imply that specific point measurements of DSW can be spatially representative for larger scale variability of DSW through the effects of cloud cover, illustrating the usefulness of surface data networks.

[45] 4. Large differences were detected across seasons for a particular chosen DSW station and these variations depended on its location. For example, the chosen DSW site of Braunschweig in central Europe (Figure 8) showed cloud cover stations with significance larger in spring and summer than in winter and autumn.

[46] This result agrees with the findings in *Chiacchio and Wild* [2010] where clouds in northern Europe, which also included Braunschweig in this particular study, mainly influence changes in DSW in spring and summer than in winter and autumn. Also, the area of significance in spring and summer closely matches the area of significance represented by the effect of the NCP circulation pattern on the DSW (Figures 15b and 15c), suggesting that the DSW in this station is attributed by the NCP and its associated cloud cover. A reasonable explanation for a weaker relationship between DSW and cloud cover in the winter and autumn could be due to the higher concentration of aerosols during the winter months when the atmosphere is more stable, which diminishes the amount of solar radiation reaching the surface during clear days [*Stjern et al.*, 2009]. Thus, this would weaken the correlation between cloud cover and DSW.

[47] 5. For a more southerly located DSW site in Klagenfurt but still considered in central Europe (Figure 9), cloud cover was more important in winter and autumn shown by its stronger significance where cloud cover is high in winter in central Europe [*Gjertsen*, 1997].

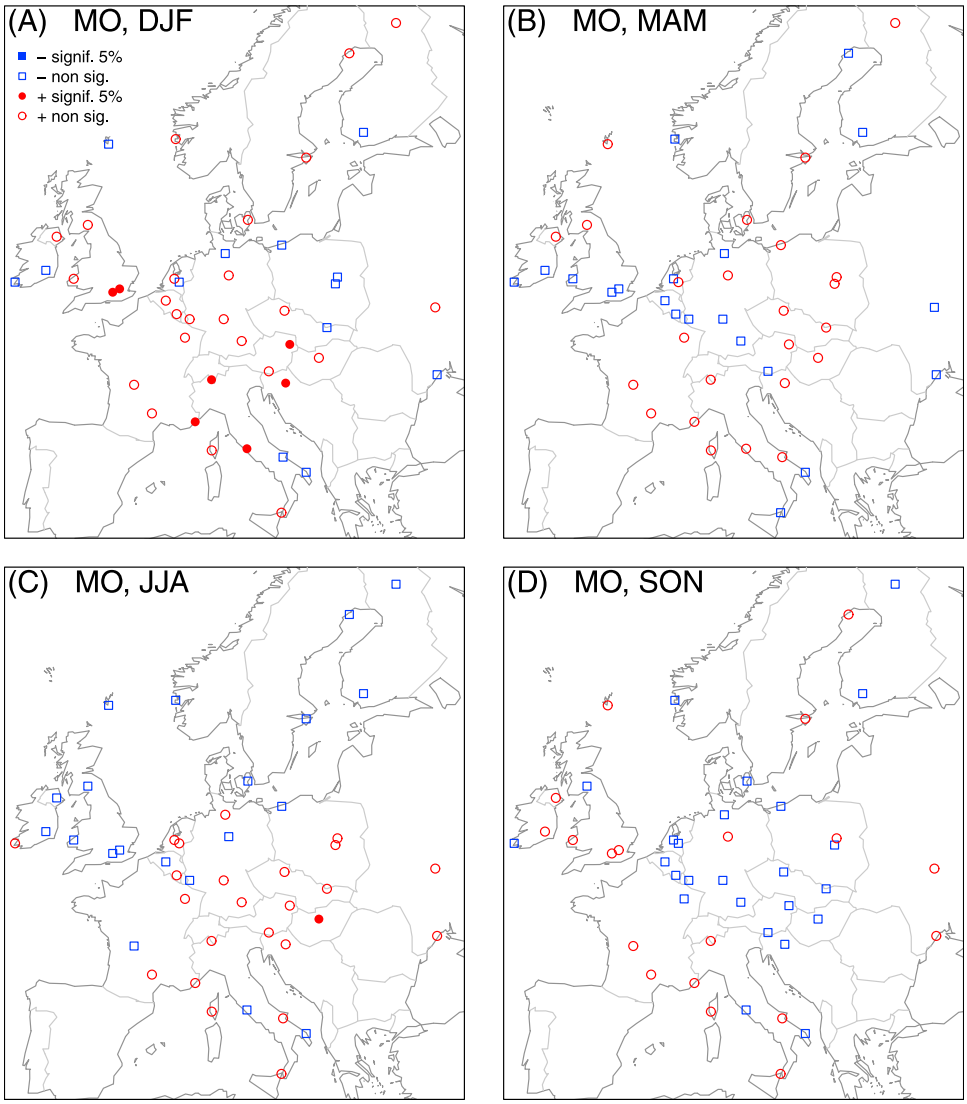

Figure 14. As in Figure 13 but for the coefficient β_2 in the individual season linear regression model (equation (7)) corresponding to the Mediterranean Oscillation (MO) index.

[48] The stronger link between DSW and cloud cover in this site during these seasons could be due to the NAO mode of variability [*Chiacchio and Wild*, 2010] where it governs variations in cloud cover [*Lolis*, 2009] and temperatures [*Castro-Díez et al.*, 2002] in southern Europe and the Mediterranean. However, in this analysis the NAO dipole structure of cloud cover did not exist with negative and positive cloud effects, which could be due the location of this station situated in an area where clear effects of the NAO on the DSW are not observed. Interestingly, the Klagenfurt station is located on the border of the region separating the dipole effect of the NAO between northern and southern Europe. This station is included in the effects of the NAO in northern Europe during 1970–1985 in winter when the NAO was primarily in its negative phase and it experiences effects of the NAO from southern Europe for 1985–2000 in winter [e.g., *Chiacchio and Wild*, 2010, Figures 5 and 7] during the period when the NAO was in its most positive phase [*Hurrell et al.*, 2003]. Hence, because our analysis covers both of these time periods it could be that the overall effect of the NAO on the DSW is diminished.

[49] 6. The NAO overall had a negative effect throughout Europe with little significance (Figure 12a). When restricted to seasons, however, the NAO more clearly displayed the dipole-like behavior in winter and less in other seasons.

[50] This shows the complex behavior of the NAO as was the case when the NAOI was compared to values of the DSW revealing both a positive and negative relationship in spring and summer and slightly positive in winter and autumn (Figure 10, middle). From the Gaussian regression model the NAO structure in winter revealed a negative effect in northern and central Europe and a positive effect in the south and is consistent to those of sunshine duration [*Pozo-Vázquez et al.*, 2004] and DSW [*Chiacchio and Wild*, 2010] and closely resembles the pattern found for cloud cover [*Trigo et al.*, 2002; *Chiacchio and Wild*, 2010] and precipitation [*Hurrell*, 1995].

[51] 7. The MO effect on DSW clearly revealed the dipole structure similar to the NAO in winter (Figure 12b). It also

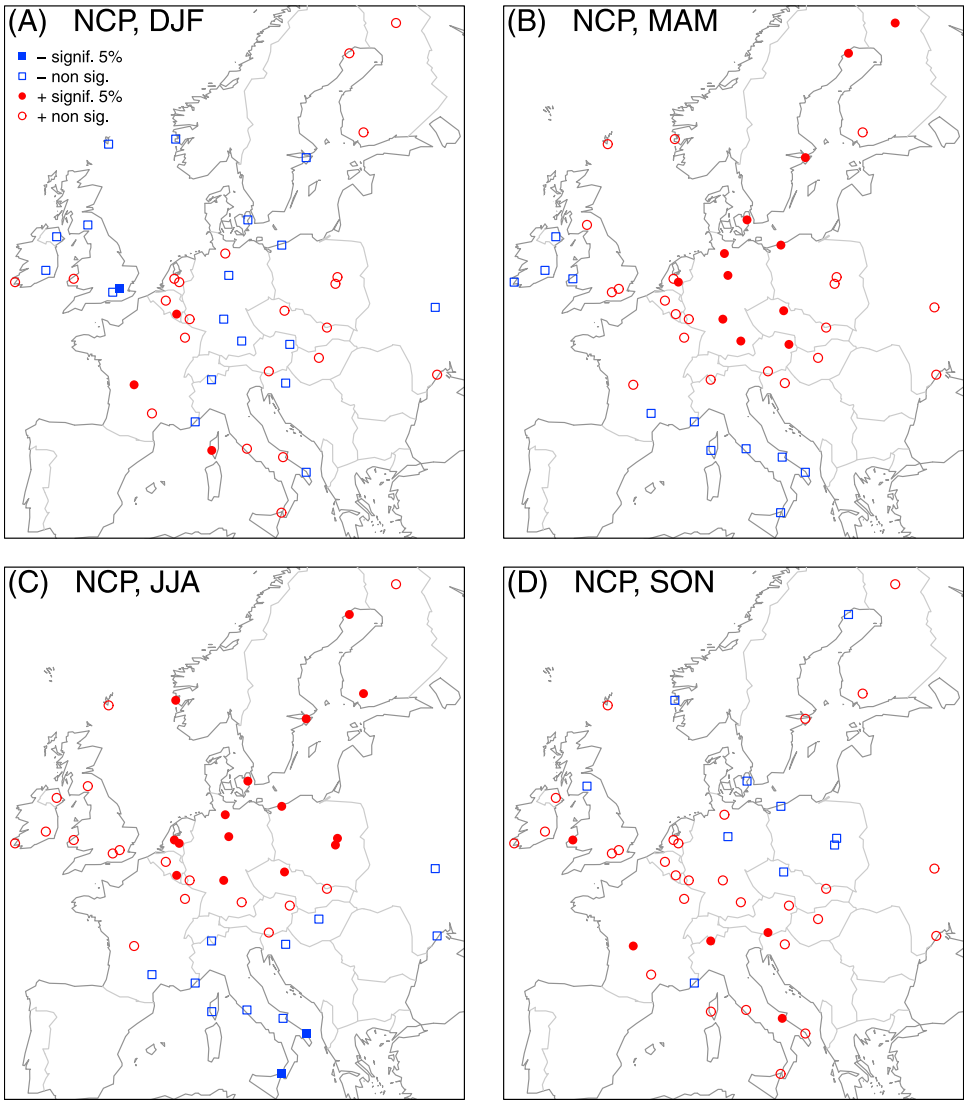

Figure 15. As in Figure 13 but for coefficient β_3 in the individual season linear regression model (equation (7)) corresponding to the North Sea Caspian Pattern (NCP) index.

showed that the MO had a statistically significant stronger effect in the south than the NAO.

[52] This may indicate that this circulation pattern plays a greater role on the DSW in the Mediterranean, which is the case for rainfall patterns [*Conte et al.*, 1989; *Corte-Real et al.*, 1995; *Maheras et al.*, 1999; *Dünkeloh and Jacobeit*, 2003]. Hence, this may also suggest that the DSW in this region may largely contribute to precipitation changes through variations in the surface radiative heating. When different seasons were analyzed, the MO had a stronger effect in winter than in other seasons, however, it no longer resembled the NAO and positive effects were mainly seen in the central to southern parts of Europe. The effect of the MO on the DSW, determined from the Gaussian regression model (Figure 14a), agrees with the positive relationship found between these two variables mainly in winter (Figure 10, left) further adding to the reliability of the GLMs applied here.

[53] 8. The NCP showed the strongest positive effect on the DSW out of the three circulation patterns analyzed primarily in spring and summer with significance in east-central to northern Europe which is in line with the location of effects from this teleconnection pattern. This also agrees with the comparison between the NCPI and DSW values where a strong positive relationship was found between these two variables (Figure 10, right) in spring and summer.

[54] These results give added confidence to the GLMs used here. Moreover, because the NCPI on average is found to be negative throughout the year with maximum values in winter and autumn and minimum in spring and summer [*Kutiel and Benaroch*, 2002], it implies a circulation pattern that is counterclockwise in the western sector (westerly circulation toward central and northern Europe) and clockwise in the eastern sector (easterly circulation toward the eastern Mediterranean) of the NCP [*Kutiel and Benaroch*, 2002, Figure 6a]. Also found in this latter study is above normal temperatures and below normal precipitation in eastern Mediterranean during more frequent negative NCP phases. Based on these findings, we could then infer from our results (i.e., Figures 15b and 15c) that the effect of the NCP on the DSW is negative during these climate conditions in this

region and positive in the east-central to northern parts of Europe where an opposite climatic pattern is possibly occurring (below average temperatures and higher than average precipitation). Our results may provide a link to be established between the circulation pattern and DSW as well as with temperature and precipitation.

[55] There has been up until now a lack of knowledge on the relationship between different circulation patterns and DSW. This study has given important results needed to establish a link between the cloud cover and atmospheric circulation patterns with the DSW on a seasonal basis, which is complementary to the well-established link between the NAO and DSW [*Pozo-Vázquez et al.*, 2004; *Chiacchio and Wild*, 2010] and many other climatic variables including surface temperature, precipitation and oceanic and ecological variables [*Hurrell et al.*, 2003]. Also, from our results we infer that the MO and NCP circulation patterns could play an important role on the decadal changes in DSW as did the NAO in *Chiacchio and Wild* [2010], which in turn can largely influence many surface processes including the hydrological and carbon cycle [*Liepert et al.*, 2004; *Wild and Liepert*, 2010; *Mercado et al.*, 2009] as well as surface temperature [*Ramanathan et al.*, 2001; *Wild et al.*, 2005, 2007]. Thus, understanding the mechanisms that govern these circulation patterns remains paramount.

[56] With a better and more detailed understanding of the effects of these climate variables and patterns on the DSW in Europe, it might help to provide a deterministic relationship when such patterns are under external anthropogenic forcing [e.g., *Osborn et al.*, 1999; *Paeth et al.*, 1999; *Ulbrich and Christoph*, 1999; *Visbeck et al.*, 2001; *Bojariu and Gimeno*, 2003; *Hurrell et al.*, 2003; *Deser and Phillips*, 2009; *Paeth and Pollinger*, 2010]. Such a relationship may enable some predictability of the variability of the circulation patterns studied, which would have important socio-economical implications, especially during the occurrence of extreme events and temperatures [*Xoplaki et al.*, 2003; *Hertig et al.*, 2010] or summer European heatwaves [*Schär et al.*, 2004; *Kuglitsch et al.*, 2010] and its consistent geographical patterns [*Fischer and Schär*, 2010]. Moreover, knowledge of a link between these circulation patterns and DSW could also improve understanding on certain feedbacks that may be associated with their low-frequency variations. Future work could involve studying these feedbacks in addition to a more clear and possible quantitative relationship between DSW, temperature and precipitation patterns.

[57] **Acknowledgments.** This research is financially supported by the ITCP. We thank the Editor Steve Ghan and the three anonymous reviewers for their comments. The authors would like to express their gratitude to Christoph Schär, Martin Wild, Atsumu Ohmura and Filippo Giorgi for their support. We thank Guido Muller and Martin Wild for their support of the GEBA database. Renato Vitolo acknowledges support by the Willis Research Network (www.willisresearchnetwork.com). Cloud cover data was obtained from the Carbon Dioxide Information Analysis Center (CDIAC) located under the United States Department of Energy at the Oak Ridge National Laboratory (http://cdiac.ornl.gov/). The NAO, MO, and NCP indices were taken from the Climate Research Unit (CRU) at the University of East Anglia in Norwich, United Kingdom (http://www.cru.uea.ac.uk/).

References

Bojariu, R., and L. Gimeno (2003), Predictability and numerical modeling of the North Atlantic Oscillation, *Earth Sci. Rev.*, *63*, 145–168, doi:10.1016/S0012-8252(03)00036–9.

Castro-Díez, Y., D. Pozo-Vázquez, F. S. Rodrigo, and M. J. Esteban-Parra (2002), NAO and winter temperature variability in southern Europe, *Geophys. Res. Lett.*, *29*(8), 1160, doi:10.1029/2001GL014042.

Cermak, J., M. Wild, R. Knutti, M. I. Mishchenko, and A. K. Heidinger (2010), Consistency of global satellite-derived aerosol and cloud data sets with recent brightening observations, *Geophys. Res. Lett.*, *37*, L21704, doi:10.1029/2010GL044632.

Chiacchio, M., and M. Wild (2010), Influence of NAO and clouds on long-term seasonal variations of surface solar radiation in Europe, *J. Geophys. Res.*, *115*, D00D22, doi:10.1029/2009JD012182.

Chiacchio, M., T. Ewen, M. Wild, and E. Arabini (2010), Influence of climate shifts on decadal variations of surface solar radiation in Alaska, *J. Geophys. Res.*, *115*, D00D21, doi:10.1029/2009JD012533.

Chiacchio, M., T. Ewen, M. Wild, M. Chin, and T. Diehl (2011), Decadal variability of aerosol optical depth in Europe and its relationship to the temporal shift of the North Atlantic Oscillation in the realm of dimming and brightening, *J. Geophys. Res.*, *116*, D02108, doi:10.1029/2010JD014471.

Conte, M., A. Giufrida, and S. Tedesco (1989), The Mediterranean oscillation, in *Impact on Precipitation and Hydrology in Italy Climate Water*, pp. 121–137, Acad. of Finland, Helsinki.

Corte-Real, J., X. Zhang, and X. Wang (1995), Large-scale circulation regimes and surface climatic anomalies over the Mediterranean, *Int. J. Climatol.*, *15*, 1135–1150, doi:10.1002/joc.3370151006.

Deser, C., and A. Phillips (2009), Atmospheric circulation trends, 1950–2000: The relative roles of sea surface temperature forcing and direct atmospheric radiative forcing, *J. Clim.*, *22*, 396–413, doi:10.1175/2008JCLI2453.1.

Dünkeloh, A., and J. Jacobeit (2003), Circulation dynamics of Mediterranean precipitation variability 1948–1998, *Int. J. Climatol.*, *23*, 1843–1866, doi:10.1002/joc.973.

Fischer, E. M., and C. Schär (2010), Consistent geographical patterns of changes in high-impact European heatwaves, *Nat. Geosci.*, *3*, 398–403, doi:10.1038/ngeo866.

Gilgen, H., and A. Ohmura (1999), The Global Energy Balance Archive, *Bull. Am. Meteorol. Soc.*, *80*(5), 831–850, doi:10.1175/1520-0477(1999)080<0831:TGEBA>2.0.CO;2.

Gilgen, H., M. Wild, and A. Ohmura (1998), Means and trends of shortwave irradiance at the surface estimated from Global Energy Balance Archive Data, *J. Clim.*, *11*, 2042–2061, doi:10.1175/1520-0442-11.8.2042.

Gillett, N. P., H. F. Graf, and T. J. Osborn (2003), Climate change and the North Atlantic Oscillation, in *The North Atlantic Oscillation: Climatic Significance and Environmental Impact*, *Geophys. Monogr. Ser.*, vol. 134, edited by J. W. Hurrell et al., pp. 193–209, AGU, Washington, D. C., doi:10.1029/134GM09.

Giorgi, F. (2006), Climate change hot-spots, *Geophys. Res. Lett.*, *33*, L08707, doi:10.1029/2006GL025734.

Gjertsen, U. (1997), The seasonal variation of cloud parameters over central Europe: A fuzzy approach for the analysis of NOAA-APT data, *Atmos. Res.*, *45*, 123–152, doi:10.1016/S0169-8095(97)00023-9.

Hahn, C. J., and S. G. Warren (2003), Cloud climatology for land stations worldwide, 1971–1996, *Numer. Data Package NDP-026D*, Carbon Dioxide Inf. Anal. Cent., Dep. of Energy, Oak Ridge, Tenn.

Hatzianastassiou, N., C. Matsoukas, E. Drakakis, P. W. Stackhouse Jr., P. Koepke, A. Fotiadi, K. G. Pavlakis, and I. Vardavas (2007), The direct effect of aerosols on solar radiation based on satellite observations, reanalysis datasets, and spectral aerosol optical properties from Global Aerosol Data Set (GADS), *Atmos. Chem. Phys.*, *7*, 2585–2599, doi:10.5194/acp-7-2585-2007.

Hertig, E., S. Seubert, and J. Jacobeit (2010), Temperature extremes in the Mediterranean area: Trends in the past and assessment for the future, *Nat. Hazards Earth Syst. Sci.*, *10*, 2039–2050, doi:10.5194/nhess-10-2039-2010.

Hurrell, J. W. (1995), Decadal trends in the North Atlantic Oscillation: Regional temperatures and precipitation, *Science*, *269*, 676–679, doi:10.1126/science.269.5224.676.

Hurrell, J. W., Y. Kushnir, M. Visbeck, and G. Ottersen (2003), An overview of the North Atlantic Oscillation, in *The North Atlantic Oscillation: Climate Significance and Environmental Impact*, *Geophys. Monogr. Ser.*, vol. 134, edited by J. W. Hurrell et al., pp. 1–35, AGU, Washington, D. C.

Hurrell, J. W., et al. (2006), Atlantic climate variability and predictability: A CLIVAR perspective, *J. Clim.*, *19*, 5100–5121, doi:10.1175/JCLI3902.1.

Jones, P. D., T. Jónsson, and D. Wheeler (1997), Extension to the North Atlantic Oscillation using early instrumental pressure observations from Gibraltar and south-west Iceland, *Int. J. Climatol.*, *17*, 1433–1450, doi:10.1002/(SICI)1097-0088(19971115)17:13<1433::AID-JOC203>3.0.CO;2-P.

Kuglitsch, F. G., A. Toreti, E. Xoplaki, P. M. Della-Marta, C. S. Zerefos, M. Türkeş, and J. Luterbacher (2010), Heat wave changes in the eastern Mediterranean since 1960, *Geophys. Res. Lett.*, *37*, L04802, doi:10.1029/2009GL041841.

Kutiel, H., and Y. Benaroch (2002), North Sea–Caspian Pattern (NCP)—An upper level atmospheric teleconnection affecting the eastern Mediterranean: Identification and definition, *Theor. Appl. Climatol.*, *71*, 17–28, doi:10.1007/s704-002-8205-x.

Liepert, B. G. (2002), Observed reductions of surface solar radiation at sites in the United States and worldwide from 1961 to 1990, *Geophys. Res. Lett.*, *29*(10), 1421, doi:10.1029/2002GL014910.

Liepert, B. G., J. Feichter, U. Lohmann, and E. Roeckner (2004), Can aerosols spin down the water cycle in a warmer and moister world?, *Geophys. Res. Lett.*, *31*, L06207, doi:10.1029/2003GL019060.

Lolis, C. J. (2009), Winter cloudiness variability in the Mediterranean region and its connection to atmospheric circulation features, *Theor. Appl. Climatol.*, *96*, 357–373, doi:10.1007/s00704-008-0046-0.

Maheras, P., E. Xoplaki, T. Davies, J. Martin-Vide, M. Bariendos, and M. J. Elkoforado (1999), Warm and cold monthly anomalies across the Mediterranean basin and their relationship with circulation: 1860–1990, *Int. J. Climatol.*, *19*, 1697–1715, doi:10.1002/(SICI)1097-0088(199912)19:15<1697::AID-JOC442>3.0.CO;2-S.

Mariotti, A., and P. Arkin (2006), The North Atlantic Oscillation and oceanic precipitation variability, *Clim. Dyn.*, *28*(1), 35–51, doi:10.1007/s00382-006-0170-4.

McCullagh, P., and J. Nelder (1989), *Generalized Linear Models*, 2nd ed., CRC, Boca Raton, Fla.

Mercado, L. M., N. Bellouin, S. Sitch, O. Boucher, C. Huntingford, M. Wild, and P. M. Cox (2009), Impact of changes in diffuse radiation on the global land carbon sink, *Nature*, *458*, 1014–1017, doi:10.1038/nature07949.

Norris, J. R., and M. Wild (2007), Trends in aerosol radiative effects over Europe inferred from observed cloud cover, solar "dimming," and solar "brightening," *J. Geophys. Res.*, *112*, D08214, doi:10.1029/2006JD007794.

Osborn, T. J., K. R. Briffa, S. F. B. Tett, P. D. Jones, and R. M. Trigo (1999), Evaluation of the North Atlantic Oscillation as simulated by a coupled climate model, *Clim. Dyn.*, *15*, 685–702, doi:10.1007/s003820050310.

Paeth, H., and F. Pollinger (2010), Enhanced evidence in climate models for changes in extratropical atmospheric circulation, *Tellus, Ser. A*, *62*, 647–660.

Paeth, H., A. Hense, R. Glowienka-Hense, and R. Voss (1999), The North Atlantic Oscillation as an indicator for greenhouse-gas induced regional climate change, *Clim. Dyn.*, *15*, 953–960, doi:10.1007/s003820050324.

Pinker, R. T., B. Zhang, and E. G. Dutton (2005), Do satellites detect trends in surface solar radiation?, *Science*, *308*, 850–854, doi:10.1126/science.1103159.

Pozo-Vázquez, D., J. Tovar-Pescador, S. R. Gámiz-Fortis, M. J. Esteban-Parra, and Y. Castro-Díez (2004), NAO and solar radiation variability in the European North Atlantic region, *Geophys. Res. Lett.*, *31*, L05201, doi:10.1029/2003GL018502.

Quadrelli, R., and J. M. Wallace (2004), A simplified linear framework for interpreting patterns of Northern Hemisphere wintertime climate variability, *J. Clim.*, *17*, 3728–3744, doi:10.1175/1520-0442(2004)017<3728:ASLFFI>2.0.CO;2.

Ramanathan, V., P. J. Crutzen, J. T. Kiehl, and D. Rosenfeld (2001), Aerosols, climate, and the hydrological cycle, *Science*, *294*(5549), 2119–2124, doi:10.1126/science.1064034.

Rauthe, M., and H. Paeth (2004), Relative importance of Northern Hemisphere circulation modes in predicting regional climate change, *J. Clim.*, *17*, 4180–4189, doi:10.1175/JCLI3140.1.

Ruckstuhl, C., et al. (2008), Aerosol and cloud effects on solar brightening and the recent rapid warming, *Geophys. Res. Lett.*, *35*, L12708, doi:10.1029/2008GL034228.

Sanchez-Lorenzo, A., J. Calbo, and J. Martin-Vide (2008), Spatial and temporal trends in sunshine duration over western Europe (1938–2004), *J. Clim.*, *21*(22), 6089–6098, doi:10.1175/2008JCLI2442.1.

Schär, C., P. L. Vidale, D. Luthi, C. Frei, C. Haberli, M. A. Liniger, and C. Appenzeller (2004), The role of increasing temperature variability in European summer heatwaves, *Nature*, *427*, 332–336, doi:10.1038/nature02300.

Semenov, V., M. Latif, J. Jungclaus, and W. Park (2008), Is the observed NAO variability during the instrumental record unusual?, *Geophys. Res. Lett.*, *35*, L11701, doi:10.1029/2008GL033273.

Stanhill, G., and S. Cohen (2001), Global dimming: A review of the evidence for a widespread and significant reduction in global radiation with a discussion of its probable causes and possible agricultural consequences, *Agric. For. Meteorol.*, *107*, 255–278, doi:10.1016/S0168-1923(00)00241-0.

Stephenson, D. B., V. Pavan, M. Collins, M. M. Junge, and R. Quadrelli (2006), North Atlantic Oscillation response to transient greenhouse gas forcing and the impact on European winter climate: A CMIP2 multi-model assessment, *Clim. Dyn.*, *27*, 401–420, doi:10.1007/s00382-006-0140-x.

Stjern, C. W., J. E. Kristjansson, and A. W. Hansen (2009), Global dimming and global brightening—An analysis of surface radiation and cloud cover data in northern Europe, *Int. J. Climatol.*, *29*, 643–653, doi:10.1002/joc.1735.

Suselj, K., and K. Bergant (2006), Mediterranean Oscillation Index, *Geophys. Res. Abstr.*, *8*, 02145.

Thompson, D. W. J., and J. M. Wallace (2001), Regional climate impacts of the Northern Hemisphere Annular Mode, *Science*, *293*, 85–89, doi:10.1126/science.1058958.

Trigo, R. M., T. J. Osborn, and J. Corte-Real (2002), The North Atlantic Oscillation influence on Europe: Climate impacts and associated physical mechanisms, *Clim. Res.*, *20*, 9–17, doi:10.3354/cr020009.

Ulbrich, U., and M. Christoph (1999), A shift of the NAO and increasing storm track activity over Europe due to anthropogenic greenhouse gas forcing, *Clim. Dyn.*, *15*, 551–559, doi:10.1007/s003820050299.

Visbeck, M. H., J. W. Hurrell, L. Polvani, and H. M. Cullen (2001), The North Atlantic Oscillation: Past, present, and future, *Proc. Natl. Acad. Sci. U. S. A.*, *98*(23), 12,876–12,877, doi:10.1073/pnas.231391598.

Warren, S. G., and C. J. Hahn (2002), Cloud climatology, in *Encyclopedia of Atmospheric Sciences*, pp. 476–483, Oxford Univ. Press, New York.

Wild, M. (2009), Global dimming and brightening: A review, *J. Geophys. Res.*, *114*, D00D16, doi:10.1029/2008JD011470.

Wild, M., and B. Liepert (2010), The Earth radiation balance as driver of the global hydrological cycle, *Environ. Res. Lett.*, *5*, 025203, doi:10.1088/1748-9326/5/2/025203.

Wild, M., H. Gilgen, A. Roesch, A. Ohmura, C. Long, E. Dutton, B. Forgan, A. Kallis, V. Russak, and A. Tsvetkov (2005), From dimming to brightening: Decadal changes in solar radiation at the Earth's surface, *Science*, *308*(5723), 847–850, doi:10.1126/science.1103215.

Wild, M., A. Ohmua, and K. Makowski (2007), Impact of global dimming and brightening on global warming, *Geophys. Res. Lett.*, *34*, L04702, doi:10.1029/2006GL028031.

Xoplaki, E., J. F. Gonzalez-Rouce, J. Luterbacher, and H. Warner (2003), Mediterranean summer air temperature variability and its connection to the large-scale atmospheric circulation and SSTs, *Clim. Dyn.*, *20*(7–8), 723–739, doi:10.1007/s00382-003-0304-x.